Rigid-Body Attitude Control

USING ROTATION MATRICES FOR CONTINUOUS, SINGULARITY-FREE CONTROL LAWS

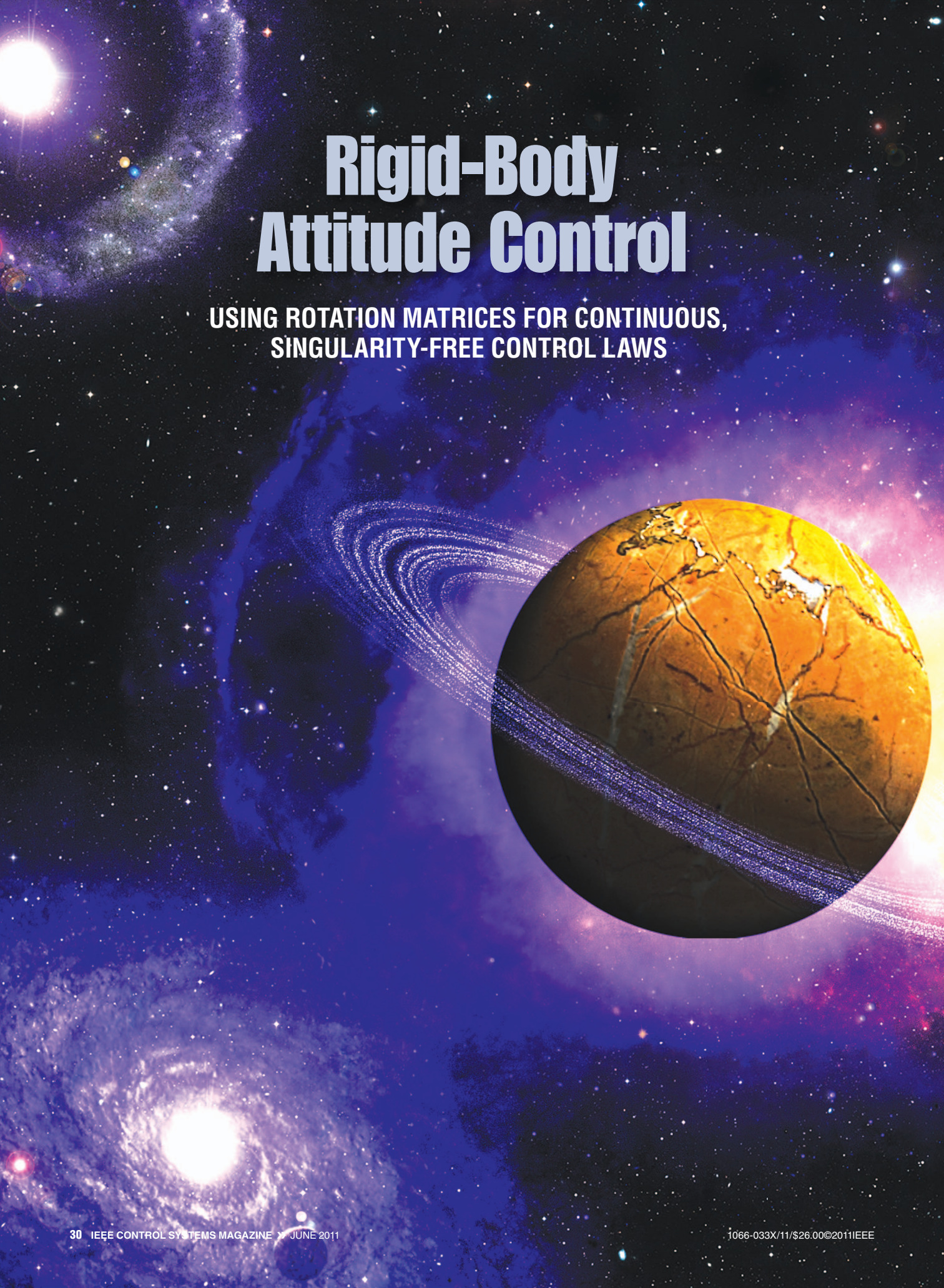

1066-033X/11/$26.00©2011IEEE

Rigid-body attitude control is motivated by aerospace applications that involve attitude maneuvers or attitude stabilization. In addition to spacecraft and atmospheric flight vehicles, applications of rigid-body attitude control arise for underwater vehicles, ground vehicles, and robotic systems. The set of attitudes of a rigid body is the set of 3×3 orthogonal matrices whose determinant is one. This set is the configuration space of rigid-body attitude motion; however, this configuration space is not Euclidean. Since the set of attitudes is not a Euclidean space, attitude control is typically studied using various attitude parameterizations [1]–[8]. These parameterizations can be Euclidean, as in the case of Euler angles, which lie in $\mathbb{R}^3$, or non-Euclidean, as in the case of quaternions, which lie in the non-Euclidean three-sphere $\mathbb{S}^3$.

Regardless of the choice of parameterization, all parameterizations [1], [2] fail to represent the set of attitudes both globally and uniquely. For example, although Euler angles can represent every attitude, this representation is not unique at certain attitudes. In fact, the time derivatives of the Euler angles at these attitudes cannot represent every possible angular velocity. The term *gimbal lock* is used to describe this mathematical singularity. Along the same lines, quaternions can represent all possible attitudes and angular velocities, but this representation is not unique; see "Representations of Attitude" for more details. Since parameterizations such as Euler angles and quaternions are unable to represent the set of attitudes both globally and uniquely, results obtained with these parameterizations have to be reinterpreted on the set of attitudes described by orthogonal matrices. Neglecting this analysis can result in undesirable behavior such as *unwinding* [9], which refers to the unstable behavior of a closed-loop attitude control system. In particular, for certain initial conditions, the trajectories of the closed-loop system start close to the desired attitude equilibrium in state space and yet travel a large distance in the state space before returning to the desired attitude. This closed-loop trajectory is analogous to the homoclinic orbit observed in a simple pendulum that swings 360° when perturbed from its inverted position at rest. Unwinding can result in wasted control effort by causing the rigid body to perform a large-angle slew maneuver when a small-angle slew maneuver in the opposite rotational direction is sufficient to achieve the objective; see "Pitfalls of Using Quaternion Representations for Attitude Control" for a description and illustration of unwinding in attitude control using quaternions.

NALIN A. CHATURVEDI, AMIT K. SANYAL, and N. HARRIS McCLAMROCH

Digital Object Identifier 10.1109/MCS.2011.940459
Date of publication: 16 May 2011

Motivated by the desire to represent attitude both globally and uniquely in the analysis of rigid-body rotational motion, this article uses orthogonal matrices exclusively to represent attitude and to develop results on rigid-body attitude control. An advantage of using orthogonal matrices is that these control results, which include open-loop attitude control maneuvers and stabilization using continuous feedback control, do not require reinterpretation on the set of attitudes viewed as orthogonal matrices. The main objective of this article is to demonstrate how to characterize properties of attitude control systems for arbitrary attitude maneuvers without using attitude parameterizations.

DESCRIPTIONS OF RIGID-BODY ATTITUDE CONFIGURATIONS

The attitude of a rigid body can be modeled by a linear transformation between a reference frame and a body-fixed frame that preserves the distance between each pair of material points in the body and the handedness of coordinate frames [1], [2], [6], [10]–[13]. Assuming each frame is defined by three orthogonal unit vectors ordered according to the right-hand rule, the attitude of the rigid body, as a linear transformation, is represented by a 3×3 matrix that transforms a vector resolved in the body-fixed frame into its representation resolved in the reference frame. The three column vectors of the matrix represent the three orthogonal unit basis vectors of the body-fixed frame resolved in the reference frame. Likewise, the three rows of the matrix represent the three orthogonal unit basis vectors of the reference frame resolved in the body frame. The resulting matrix, referred to as a rotation matrix, represents the physical attitude of the rigid body. The set of all rotation matrices is the *special orthogonal* group of rigid rotations in $\mathbb{R}^3$, which is denoted by $\mathrm{SO}(3)$; see "Attitude Set Notation" for a definition of these and additional related sets.

In rigid-body pointing applications, the rotation about the pointing direction is irrelevant since these rotations do not change the direction in which the body points. Thus, while rotation matrices $R \in \mathrm{SO}(3)$ can be used to model the attitude of a rigid body, not all the information available in the rotation matrix is required for pointing applications. In this case, a reduced representation of the rotation matrix can be used for pointing applications. An example of such a reduced representation is the reduced-attitude vector [14]. To develop the reduced-attitude vector representation of a rigid body, suppose $b \in \mathbb{S}^2$, where $\mathbb{S}^2$ is the unit sphere in three-dimensional space, is a unit vector that denotes a fixed pointing direction specified in the reference frame. Then, in the body-fixed frame, this direction vector can be expressed as $\Gamma \triangleq R^{\mathrm{T}} b \in \mathbb{S}^2$, where R^{T} denotes the transpose of the rotation matrix R

Representations of Attitude

Rigid body attitude is often represented using three or four parameters. Unit quaternions and the axis-angle representation use four parameters to represent the attitude. Three-parameter representations of attitude include the Euler angles as well as parameters derived from the unit quaternions as in the case of the Rodrigues parameters and the modified Rodrigues parameters. These three-parameter sets can be viewed as embedded subsets of $\mathbb{R}^3$, thus allowing methods of analysis that are suited to the Euclidean space $\mathbb{R}^3$. Euler angles are kinematically singular since the transformation from their time rates of change to the angular velocity vector is not globally defined. The Rodrigues parameters and modified Rodrigues parameters are geometrically singular since they are not defined for 180° of rotation. Therefore, continuous control laws using these three-parameter representations cannot be globally defined, and, as such, these representations are limited to local attitude maneuvers.

Table S1 presents various attitude representations and their key properties. While the quaternions, axis-angle variables, and rotation matrices can represent all attitudes of a rigid body, only rotation matrices can represent all attitudes uniquely.

Table S1 Properties of attitude representations.

Attitude Representation	Global?	Unique?
Euler angles	No	No
Rodrigues parameters	No	No
Modified Rodrigues parameters	No	No
Quaternions	Yes	No
Axis-angle	Yes	No
Rotation matrix	Yes	Yes

As shown in Table S1, since the unit quaternions are global in their representation of attitude, they are often used in practical applications to represent rigid-body attitude. However, note that the map from the space $\mathbb{S}^3$ of unit quaternions to the space $\mathrm{SO}(3)$ of rotations is not unique. In particular, this map is a two-fold covering map, where each physical attitude $R \in \mathrm{SO}(3)$ is represented by a pair of antipodal unit quaternions $\pm q \in \mathbb{S}^3$. If not carefully designed, quaternion-based controllers may yield undesirable phenomena such as unwinding [9]; see "Pitfalls of Using Quaternion Representations for Attitude Control" for more details.

representing the attitude of the rigid body. We refer to the vector Γ as the reduced-attitude vector of the rigid body. Thus, a reduced-attitude vector describes a direction b fixed in the reference frame by a unit vector resolved in the body frame. In pointing applications, a pointing direction $b \in \mathbb{S}^2$ in the reference frame can be expressed by the reduced attitude Γ corresponding to b, and, hence, the reduced attitude can be used to study pointing applications for a rigid body.

FULL- AND REDUCED-ATTITUDE CONTROL

Rigid-body attitude control problems can be formulated in terms of attitude configurations defined in $\mathrm{SO}(3)$ or in terms of reduced-attitude configurations defined in $\mathbb{S}^2$. The former case involves control objectives stated directly in terms of the full attitude of the rigid body, while the latter case involves control objectives stated in terms of pointing the rigid body. In particular, the latter case is used when the control objectives can be formulated in terms of pointing a body-fixed imager, antenna, or other instrument in a specified direction in the reference frame, where rotations about that specified body-fixed direction are irrelevant.

We subsequently study several full-attitude and reduced-attitude control problems. In each case, we begin by treating open-loop attitude control problems defined by specifying initial conditions, terminal conditions, and a maneuver time. Then we treat attitude-stabilization problems using continuous feedback control. In particular, we seek continuous attitude control laws that modify the dynamics of the spacecraft such that a specified attitude or reduced attitude is rendered asymptotically stable. For full-attitude control, this continuous feedback function is defined in terms of the full rigid-body attitude and angular velocity, while, for reduced-attitude control, this feedback function is defined in terms of the reduced attitude and angular velocity.

LOCAL AND GLOBAL ATTITUDE CONTROL ISSUES

Since attitude control problems are nonlinear control problems, these problems can be categorized into local attitude control issues and global attitude control issues. In brief, local control issues address changes in the rigid-body attitude and angular velocity that lie in an open neighborhood of the desired attitude and angular velocity. Local attitude control problems typically arise when the rigid body has a limited range of rotational motion. In this case, linear control methods or local nonlinear control methods based on a convenient attitude representation may suffice, so long as no singularities occur within the local range of attitude motion of interest.

In contrast to local attitude control, global attitude control issues arise when arbitrary changes in the rigid-body attitude and angular velocity are allowed. In this case, no a priori restrictions are placed on the

possible rotational motion, and nonlinear methods are required to address these rotational motions. Global attitude control issues are motivated by applications to highly maneuverable rigid-body systems that may undergo extreme attitude changes such as rigid-body tumbling.

COMMENTS ON THE ATTITUDE CONTROL LITERATURE

The literature on attitude control can be divided into two categories. In the first category, attitude control is studied within a geometric framework, as presented in this article, by viewing rigid-body attitude as an element of $\mathrm{SO}(3)$ or $\mathbb{S}^2$ [14]–[27]. In the second category [3]–[8], [28], [29], attitude control is studied using representations of attitude in $\mathbb{R}^3$ or $\mathbb{S}^3 \subset \mathbb{R}^4$ [1], [2].

Almost-global attitude stabilization of a rigid body, in contrast to global attitude stabilization, is motivated by the fact that there exists no continuous time-invariant feedback that globally asymptotically stabilizes a single equilibrium attitude [16]–[18]. This property is related to the fact that every continuous time-invariant closed-loop vector field on $\mathrm{SO}(3)$ and $\mathbb{S}^2$ has more than one closed-loop equilibrium, and hence, the desired equilibrium cannot be globally attractive [9]; see "The Impossibility of Global Attitude Stabilization Using Continuous Time-Invariant Feedback" for more details. While [24] treats local attitude stabilization and H_∞ attitude performance issues, [19]–[23] present results for various almost-global stabilization problems for the 3D pendulum; the 3D pendulum has the same rigid-body attitude dynamics as in this article, but the moment due to uniform gravity is also included [30], [31]. This same perspective is used in [25] and [26], where results on almost-global tracking of desired attitude trajectories are presented. Rigid-body reduced-attitude control is studied in [14], [15], [22], [23], [27], and [32].

An alternative approach to attitude control based on the geometry of $\mathrm{SO}(3)$ or $\mathbb{S}^2$ is to use representations of attitude in $\mathbb{R}^3$ or $\mathbb{S}^3 \subset \mathbb{R}^4$ [1], [2], such as Euler angles, Euler parameters, or quaternions, Rodrigues parameters, and modified Rodrigues parameters [3]–[8], [15], [28], [29], [33]. While these representations can be used for local attitude control, global results obtained by using this approach must be interpreted on the configuration space $\mathrm{SO}(3)$ of the physical rigid body. Indeed, the global dynamics of the parameterized closed-loop attitude motion on $\mathbb{R}^3$ or $\mathbb{S}^3$, such as global or almost global asymptotic stability, do not necessarily imply that these closed-loop properties also hold for the dynamics of the physical rigid body evolving on the configuration space $\mathrm{SO}(3)$. Issues related to continuous attitude control using these alternative representations of attitude are described in "Representations of Attitude" and "Pitfalls of Using Quaternion Representations for Attitude Control."

FRAMEWORK FOR DESCRIBING ATTITUDE MOTION

The space of rigid-body rotations $\mathrm{SO}(3)$ is a Lie group [34], [35]; it has an algebraic group structure based on matrix multiplication as the group operation and a differential geometric structure as a compact smooth manifold that enables the use of calculus. Alternatively, the Lie group $\mathrm{SO}(3)$ of rigid-body rotations can be viewed as the set of isometries, or length-preserving transformations on $\mathbb{R}^3$ that leave the origin fixed and preserve the orientation, that is, handedness, of frames. Unlike $\mathrm{SO}(3)$, the space of rigid-body reduced-attitudes $\mathbb{S}^2$ is not a Lie group. However, each element in $\mathrm{SO}(3)$, as an orthogonal matrix, is a bijective mapping from $\mathbb{S}^2$ to $\mathbb{S}^2$.

Attitude Description Using Rotation Matrices

We now describe the properties of $\mathrm{SO}(3)$. Every rotation matrix $R \in \mathrm{SO}(3)$ satisfies

$$R^\top R = I = RR^\top, \quad \det(R) = 1, \tag{1}$$

where I denotes the 3×3 identity matrix, which is also the identity element of the group $\mathrm{SO}(3)$. This representation of the attitude is global and unique in the sense that each physical rigid-body attitude corresponds to exactly one rotation matrix. If $R_\mathrm{d} \in \mathrm{SO}(3)$ represents the desired attitude of a rigid body, then attitude control objectives can be described as rotating the rigid body so that its attitude R is the same as the desired attitude, that is, $R = R_\mathrm{d}$.

The tangent space at an element in the Lie group $\mathrm{SO}(3)$ consists of vectors tangent to all differentiable curves $t \to R(t) \in \mathrm{SO}(3)$ passing through that element. Thus, the tangent space at an element in $\mathrm{SO}(3)$ is the vector space of all possible angular velocities that a rigid body can attain at that attitude. This vector space is isomorphic to the tangent space at the identity element $R = I$, which is defined as the Lie algebra $\mathfrak{so}(3)$ of the Lie group $\mathrm{SO}(3)$. The algebraic structure of $\mathfrak{so}(3)$ is obtained from the defining equation $R(t)^\top R(t) = I = R(t)R(t)^\top$. Let $R(t) \in \mathrm{SO}(3)$ be a curve such that $R(0) = I$ and $\dot{R}(0) = S$, where $S \in \mathfrak{so}(3)$. Differentiating $R(t)^\top R(t) = I$ and evaluating at $t = 0$, we see that $S^\top + S = 0$, that is, S is skew symmetric. Thus, $\mathfrak{so}(3)$ is the matrix Lie algebra of 3×3 skew-symmetric matrices.

Each element of $\mathrm{SO}(3)$ can be represented by the matrix exponential [34]

$$\exp(S) = I + S + \frac{1}{2!}S^2 + \frac{1}{3!}S^3 + \cdots, \tag{2}$$

where S is in the Lie algebra $\mathfrak{so}(3)$ and $\exp(S)$ is in the Lie group. The Lie algebra $\mathfrak{so}(3)$ is isomorphic to $\mathbb{R}^3$, and this vector space isomorphism is given by

$$S = \begin{bmatrix} 0 & -s_3 & s_2 \\ s_3 & 0 & -s_1 \\ -s_2 & s_1 & 0 \end{bmatrix} \in \mathfrak{so}(3), \tag{3}$$

Pitfalls of Using Quaternion Representations for Attitude Control

Quaternion representations of attitude are often used in attitude control and stabilization to represent rigid-body attitude. Quaternions do not give rise to singularities, but they double cover the set of attitudes $\mathrm{SO}(3)$ in the sense that each attitude corresponds to two different quaternion vectors. Specifically, a physical attitude $R \in \mathrm{SO}(3)$ is represented by a pair of antipodal quaternions $\pm q \in \mathbb{S}^3$.

An implication of this nonunique representation is that closed-loop properties derived using quaternions might not hold for the dynamics of the physical rigid body on $\mathrm{SO}(3) \times \mathbb{R}^3$. Thus, almost global asymptotic stability of an equilibrium in the quaternion space $\mathbb{S}^3 \times \mathbb{R}^3$ does not guarantee almost global-asymptotic stability of the corresponding equilibrium in $\mathrm{SO}(3) \times \mathbb{R}^3$. Indeed, a property such as local asymptotic stability of the closed-loop vector field on $\mathbb{S}^3 \times \mathbb{R}^3$ holds on $\mathrm{SO}(3) \times \mathbb{R}^3$, only if the property holds for the projection of the vector field from $\mathbb{S}^3 \times \mathbb{R}^3$ to the space $\mathrm{SO}(3) \times \mathbb{R}^3$; see Figure S1.

If the projection of the closed-loop vector field from $\mathbb{S}^3 \times \mathbb{R}^3$ onto $\mathrm{SO}(3) \times \mathbb{R}^3$ is neglected during control design, then undesirable phenomena such as unwinding can occur [9]. In *unwinding*, a closed-loop trajectory in response to certain initial conditions can undergo a homoclinic-like orbit that starts close to the desired attitude equilibrium. Unwinding can occur in all continuous closed-loop attitude control systems that are designed using global parameterizations that are nonunique in their representation of $\mathrm{SO}(3)$; see "Representations of Attitude" for examples of global parameterizations that are nonunique in its representation of $\mathrm{SO}(3)$.

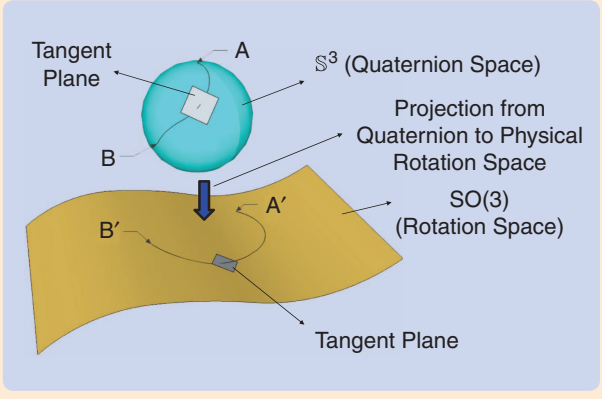

FIGURE S1 Projection of the vector field from $\mathbb{S}^3 \times \mathbb{R}^3$ to $\mathrm{SO}(3) \times \mathbb{R}^3$. Since orthogonal matrices represent the set of attitudes globally and uniquely, results obtained using alternative parameterizations of $\mathrm{SO}(3)$ have to be reinterpreted on the set of attitudes described by orthogonal matrices. Neglecting this analysis can result in undesirable behavior such as unwinding [9]. To interpret the results on $\mathrm{SO}(3)$, the closed-loop trajectory is projected from the parametric space onto $\mathrm{SO}(3)$, where the properties of the resulting closed-loop on $\mathrm{SO}(3)$ are analyzed. This figure illustrates the projection of a trajectory from the space of quaternions $\mathbb{S}^3$ onto $\mathrm{SO}(3)$.

In the case of quaternions, continuous, time-invariant state-feedback control using these representations can give rise to regions of attraction and repulsion in the neighborhood of $q \in \mathbb{S}^3$ and $-q \in \mathbb{S}^3$, respectively, where q and $-q$ represent the same desired attitude in $\mathrm{SO}(3)$. Starting from q, we can choose an initial angular velocity such that orbits connecting these regions of repulsion and attraction arise. These orbits run from a neighborhood of q to a neighborhood of $-q$ in $\mathbb{S}^3$, with a terminal velocity that is close to zero. The corresponding orbit in $\mathrm{SO}(3)$ obtained by projection as shown in Figure S1 starts and ends close to the desired attitude. However, in the quaternion space, since $-q$ has a region of repulsion, the trajectory is repelled from $-q$, eventually converging to q. In $\mathrm{SO}(3)$, the corresponding trajectory then follows a homoclinic-like orbit starting close to the desired attitude equilibrium with almost zero angular velocity, gaining velocity as the rigid body moves along the orbit, and eventually converging to the desired equilibrium. Thus, the rigid body unwinds needlessly before converging to the desired attitude. The presence of these homoclinic-like orbits in $\mathrm{SO}(3)$ indicates that, although the desired closed-loop attitude equilibrium is attractive, it is not Lyapunov stable.

To illustrate unwinding, suppose the quaternion $q \in \mathbb{S}^3$ represents the attitude of a rigid body, and let $\omega \in \mathbb{R}^3$ represent its angular velocity vector resolved in the body-fixed frame. We express $q = (q_0, \mathbf{q}_v)$, where $(q_0, \mathbf{q}_v) \in \mathbb{R} \times \mathbb{R}^3$. Then, the attitude dynamics of the rigid body in the quaternion space are given by

$$J\dot{\omega} = J\omega \times \omega + u,$$
$$\dot{q} = -\frac{1}{2}\mathbf{q}_v^{\mathrm{T}}\omega,$$
$$\dot{\mathbf{q}}_v = \frac{1}{2}(qI + \mathbf{q}_v^{\times})\omega,$$

where J is the moment of inertia matrix, I is the 3×3 identity matrix, and $u \in \mathbb{R}^3$ is the applied control input. Next, consider the PD-type control law $u(q, \omega) \triangleq -k_p\mathbf{q}_v - k_d\omega$, where $k_p, k_d > 0$. It can be shown that $q_e = (1, 0, 0, 0)$ and $\omega_e = (0, 0, 0)$ is an equilibrium of the resulting closed-loop vector field. In the physical rotation space, this equilibrium corresponds to the attitude $R_e = I$ and $\omega_e = 0$. Furthermore, the closed-loop vector field yields almost global asymptotic stability for the equilibrium $(q_e, \omega_e) \in \mathbb{S}^3 \times \mathbb{R}^3$. However, almost global asymptotic stability of $(q_e, \omega_e) \in \mathbb{S}^3 \times \mathbb{R}^3$ does not imply almost global asymptotic stability for the corresponding equilibrium $(R_e, \omega_e) \in \mathrm{SO}(3) \times \mathbb{R}^3$.

To illustrate this failure, we choose $J = \mathrm{diag}(1, 1, 1)$ kg-m^2 and $(k_p, k_d) = (0.1, 0.237)$. Furthermore, choose the initial attitude $q(0) = q_e$ and initial angular velocity $\omega(0) = [360/\pi\ 0\ 0]$ °/s. The quaternion element $q_0(t)$ is shown in Figure S2(a), and the angular velocity is shown in Figure S2(b). Furthermore, Figure S2(c) shows the error in the attitude in $\mathrm{SO}(3)$ using the eigenangle

$$\Theta(t) = \cos^{-1}\frac{1}{2}(\text{trace}(R(t)) - 1) \in [0, 180],$$

which is a scalar measure of the error between R and I. Note that since $R_e = I$, it follows that $\Theta = 0°$ for $R = R_e$. For the chosen initial conditions, the eigenangle satisfies $\Theta(0) = 0°$.

As shown in Figure S2(a) and (b), the trajectory in $\mathbb{S}^3$ approaches $-q_e$ at $t = 17$ s with a small angular velocity of magnitude 0.03 °/s and is then repelled away, eventually converging to the desired attitude q_e. This closed-loop behavior is similar to the response of a simple pendulum with angular velocity damping that is swung up to the unstable inverted equilibrium starting from the stable hanging equilibrium, where the pendulum eventually converges to the stable hanging equilibrium. Since $(q_e, 0) \in \mathbb{S}^3 \times \mathbb{R}^3$ is a stable equilibrium and $(-q_e, 0) \in \mathbb{S}^3 \times \mathbb{R}^3$ is an unstable equilibrium of the closed-loop dynamics, the closed-loop trajectory in $\mathbb{S}^3 \times \mathbb{R}^3$ shows a closed-loop response similar to the simple pendulum swinging up with angular velocity damping.

However, when the closed-loop trajectory in $\mathbb{S}^3 \times \mathbb{R}^3$ is projected onto $\text{SO}(3) \times \mathbb{R}^3$, parts (b) and (c) of Figure S2 show that the corresponding trajectory in $\text{SO}(3) \times \mathbb{R}^3$ unwinds. Thus, the closed-loop trajectory approaches the desired attitude R_e ($\Theta(t) \approx 2.75°$) with a small angular velocity ($\|\omega(t)\| \approx 0.03$ °/s) at $t = 17$ s, and yet instead of converging to the equilibrium attitude R_e, the trajectory is repelled away from $(R_e, 0)$ with an increasing angular velocity. Indeed, $\Theta(t)$ in Figure S2(c) increases to 180° at $t \approx 50$ s, eventually converging to zero. Thus, starting at $t = 17$ s, we observe a homoclinic-like orbit in $\text{SO}(3) \times \mathbb{R}^3$ at $(R_e, 0)$, which violates the stability of the equilibrium. The presence of this homoclinic-like trajectory indicates that, while the desired equilibrium is globally attractive in $\text{SO}(3) \times \mathbb{R}^3$, it is not Lyapunov stable and, hence, not asymptotically stable in $\text{SO}(3) \times \mathbb{R}^3$.

In the above example, the controller $u(q, \omega) \triangleq -k_p q_v - k_d \omega$ fails to achieve asymptotic stability on the physical space $\text{SO}(3) \times \mathbb{R}^3$ since it does not satisfy $u(q, \omega) = u(-q, \omega)$. Thus, while q and $-q$ in the quaternion space represent the same physical attitude in SO(3) the control input $u(q, \omega) \neq u(-q, \omega)$. Therefore, for each $(R, \omega) \in \text{SO}(3) \times \mathbb{R}^3$, where $R \neq R_e$, the controller yields two distinct control inputs. Hence, the projection of the closed-loop vector field from $\mathbb{S}^3 \times \mathbb{R}^3$ to $\text{SO}(3) \times \mathbb{R}^3$ yields a multivalued map. Thus, while the quaternion-based controller results in a closed-loop system that is a continuous vector field on $\mathbb{S}^3 \times \mathbb{R}^3$, the projected closed-loop system on the physical space $\text{SO}(3) \times \mathbb{R}^3$ is not a vector field. Since the projected closed loop on $\text{SO}(3) \times \mathbb{R}^3$ is not a vector field, we cannot conclude that closed-loop properties on $\mathbb{S}^3 \times \mathbb{R}^3$, such as asymptotic stability and almost global-asymptotic stability, imply the same on $\text{SO}(3) \times \mathbb{R}^3$.

In practical applications, unwinding is often resolved by changing the sign of the quaternion vector as the closed-loop

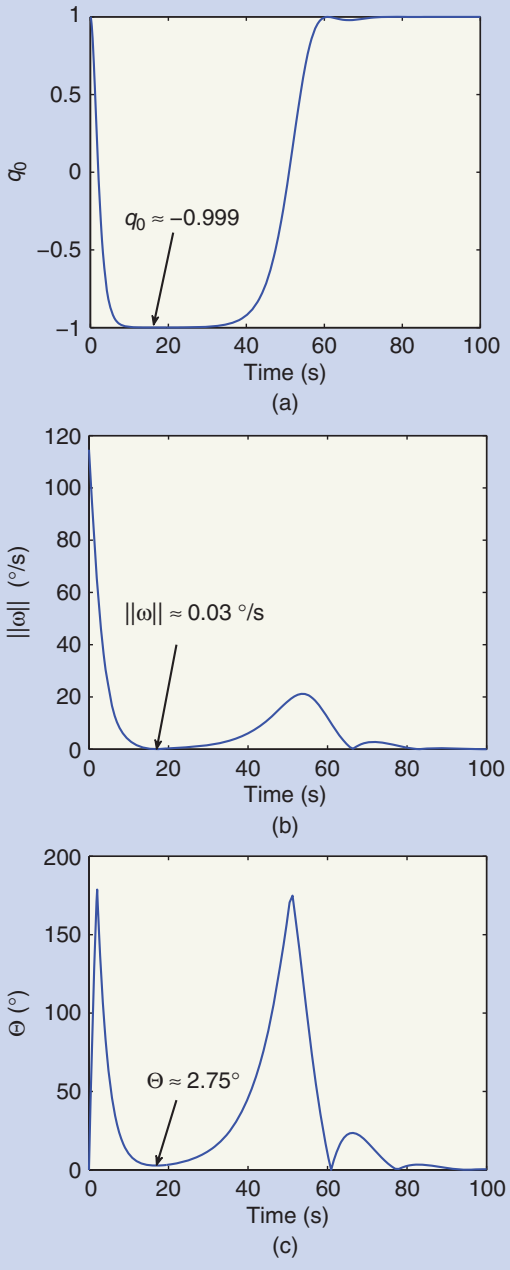

FIGURE S2 Closed-loop response of the rigid body as observed in $\mathbb{S}^3$ and SO(3). As shown in (b) and (c), the rigid body approaches the desired attitude ($\Theta = 2.75°$) with an angular velocity whose magnitude is approximately 0.03 °/s. Thus, from asymptotic stability, we expect the trajectory to converge to the desired equilibrium $(R_e, 0)$. On the contrary, the trajectory is repelled from $(R_e, 0)$, with an increasing angular velocity. This homoclinic-like orbit occurs since q in (a) approaches the unstable attitude $-q_e$ and is subsequently repelled away, converging eventually to q_e. However, in the configuration space SO(3), both q_e and $-q_e$ correspond to the same attitude and hence the homoclinic-like orbit. This phenomenon is termed unwinding.

trajectory passes from one hemisphere to the other. Indeed, the only way to define a closed-loop vector field on $\mathrm{SO}(3) \times \mathbb{R}^3$ for a continuous time-invariant, state-feedback controller using quaternions is to choose a controller that satisfies $u(q, \omega) = u(-q, \omega)$. However, changing the sign of the quaternion vector as the closed-loop trajectory passes from one hemisphere to the other results in a discontinuous closed-loop vector field on $\mathbb{S}^3 \times \mathbb{R}^3$. Note that almost global asymptotic stability of the desired attitude for the continuous controller in $\mathbb{S}^3 \times \mathbb{R}^3$ does not imply almost global asymptotic stability of the desired attitude for the discontinuous implementation of the quaternion-based controller in $\mathbb{S}^3 \times \mathbb{R}^3$. Stability analysis for discontinuous closed-loop systems requires set-valued differential equations [41].

In contrast to analysis using quaternions, none of the above issues occur for closed-loop vector fields that are defined directly on $\mathrm{SO}(3) \times \mathbb{R}^3$ by means of rotation matrices. This property is due to the fact that, unlike quaternions, rotation matrices represent rigid-body attitudes both uniquely and globally. This uniqueness property is one of the primary motivations for studying attitude-control issues on $\mathrm{SO}(3) \times \mathbb{R}^3$ in terms of rotation matrices.

where $s = [s_1 \;\; s_2 \;\; s_3]^\mathsf{T} \in \mathbb{R}^3$. This isomorphism is expressed as $S = s^\times$. The reason for the superscript is related to the fact for every $a, b \in \mathbb{R}^3$, $[a^\times]b = a \times b$. If we identify $S \in \mathfrak{so}(3)$ as $s = \alpha a$, where $a \in \mathbb{S}^2$ and $\alpha \in \mathbb{R}$, then this isomorphism gives Euler's theorem, where $a \in \mathbb{S}^2$ is the axis of rotation and $\alpha \in \mathbb{R}$ is the angle, corresponding to the rotation matrix $\exp(S) \in \mathrm{SO}(3)$. Using this isomorphism, we can express the matrix exponential of $S \in \mathfrak{so}(3)$ by Rodrigues's formula

$$\exp(S) = I + a^\times \sin(\alpha) + (a^\times)^2 (1 - \cos(\alpha)). \tag{4}$$

Reduced-Attitude Description Using Unit Vectors in $\mathbb{R}^3$

Let $\Gamma \triangleq R^\mathsf{T} b$ denote the unit vector b that is fixed in the reference frame, resolved in the body-fixed frame. Then $\Gamma \in \mathbb{S}^2$ describes the reduced attitude of a rigid body. Let $\Gamma_\mathrm{d} = R_\mathrm{d}^\mathsf{T} b \in \mathbb{S}^2$ represent the desired pointing direction of an imager, antenna, or other instrument. Pointing in terms of reduced-attitude control objectives can then be described as rotating the rigid body so that its reduced-attitude vector Γ is aligned with the desired reduced-attitude vector Γ_d, that is $\Gamma = \Gamma_\mathrm{d}$, where both reduced-attitude vectors are resolved in the body-fixed frame. Rotation about the unit vector b does not change the reduced-attitude defined by the direction of b. Therefore, all full-body attitudes that are related by such a rotation result in the same reduced attitude.

Attitude Kinematics

We denote the attitude of a rigid body by $R \in \mathrm{SO}(3)$ relative to a reference frame. Let $\omega \in \mathbb{R}^3$ be the angular velocity of the body relative to the reference frame, resolved in the body-fixed frame. Then the full-attitude kinematics equation that gives the time rate of change of the rigid-body attitude is

$$\dot{R} = R\omega^\times, \tag{5}$$

where $\omega^\times$ is a skew-symmetric matrix as given in (3).

For the fixed reference frame direction $b \in \mathbb{S}^2$, differentiating the reduced attitude $\Gamma = R^\mathsf{T} b$ with respect to time and substituting the kinematics equation (5) for the full attitude $R \in \mathrm{SO}(3)$ yields the kinematics for the reduced attitude. Since $\omega^\times$ is skew symmetric, it follows that

$$\dot{\Gamma} = \dot{R}^\mathsf{T} b = (\omega^\times)^\mathsf{T} R^\mathsf{T} b = (\omega^\times)^\mathsf{T} \Gamma = -\omega^\times \Gamma = \Gamma \times \omega. \tag{6}$$

This kinematics equation is consistent with the fact that the reduced-attitude vector Γ evolves on $\mathbb{S}^2$. Indeed, differentiating $\|\Gamma\|^2 \triangleq \Gamma^\mathsf{T}\Gamma$ with respect to time and substituting (6) yields

$$\frac{d}{dt}(\Gamma^\mathsf{T}\Gamma) = 2\Gamma^\mathsf{T}\dot{\Gamma} = 2\Gamma^\mathsf{T}(\Gamma \times \omega) = 2\omega^\mathsf{T}(\Gamma \times \Gamma) = 0.$$

Therefore, since $\Gamma(0) \in \mathbb{S}^2$, hence $\Gamma(t) \in \mathbb{S}^2$ for every $t \geq 0$. Note that the component of the angular velocity vector ω along the vector Γ does not affect the kinematics (6).

Attitude Dynamics

We now define the attitude dynamics of a rigid body with respect to an inertial reference frame. The rate of change of the rotation matrix $R \in \mathrm{SO}(3)$ depends on the angular velocity through the kinematics given by (5). The rate of change of the angular velocity expressed in the body frame is Euler's equation for a rigid body, which is given by

$$J\dot{\omega} = J\omega \times \omega + u, \tag{7}$$

where u is the sum of external moments applied to the body resolved in the body frame. We assume that the rigid body is *fully actuated*, that is, the set of all control inputs that can be applied to the rigid body is a three-dimensional Euclidean space.

GLOBAL ATTITUDE CONTROL MANEUVERS

We now consider attitude control maneuvers that rotate the rigid body from a specified initial attitude and initial

angular velocity to a specified terminal attitude and terminal angular velocity, in a specified time period. The attitude control maneuvers are defined by describing the control moment input, the resulting attitude, and the angular velocity as functions of time over the specified time period. We consider fully actuated open-loop control problems with a control function $u{:}[0, T] \to \mathbb{R}^3$. If the initial angular velocity is zero and the terminal angular velocity is zero, then the attitude control maneuver is a rest-to-rest attitude maneuver.

Full-Attitude Maneuvers

The attitude maneuver considered here is to transfer the initial attitude $R_0 \in \mathrm{SO}(3)$ and zero initial angular velocity to the terminal attitude $R_f \in \mathrm{SO}(3)$ and zero terminal angular velocity in the fixed maneuver time $T > 0$.

According to Euler's theorem [1], there exists an axis $a \in \mathbb{S}^2$ and an angle $\alpha \in [0, 2\pi)$ that satisfy

$$e^{\alpha a^\times} = R_f R_0^{-1}. \tag{8}$$

A rest-to-rest attitude maneuver that meets the specified boundary conditions is given by

$$\begin{aligned} R(t) &= e^{\theta(t)a^\times} R_0, \\ &= [I + a^\times \sin\theta(t) + (a^\times)^2(1 - \cos\theta(t))]R_0, \qquad (9) \\ \omega(t) &= \dot\theta(t)a, \qquad (10) \\ u(t) &= \ddot\theta(t)Ja + \dot\theta(t)^2(a \times Ja), \qquad (11) \end{aligned}$$

where the rotation angle $\theta{:}[0, T] \to \mathbb{S}^1$ satisfies

$$\theta(0) = 0,\ \dot\theta(0) = 0, \tag{12}$$

$$\theta(T) = \begin{cases} \alpha, & 0 \le \alpha < \pi, \\ -2\pi + \alpha, & \pi \le \alpha < 2\pi, \end{cases} \quad \dot\theta(T) = 0. \tag{13}$$

The rotation angle $\theta(t)$ can be chosen as a linear combination of sinusoids or polynomials with coefficients selected to satisfy the initial and terminal boundary conditions (12) and (13).

Reduced-Attitude Maneuvers

We now consider a reduced-attitude maneuver that transfers an initial reduced attitude $\Gamma_0 \in \mathbb{S}^2$ and zero initial angular velocity to a terminal reduced attitude $\Gamma_f \in \mathbb{S}^2$ and zero terminal angular velocity in the fixed maneuver time $T > 0$. We follow the strategy of a rotation about an inertially fixed axis. This axis, normalized to lie in $\mathbb{S}^2$, is given by $a = \Gamma_0 \times \Gamma_f / \|\Gamma_0 \times \Gamma_f\| \in \mathbb{S}^2$ assuming Γ_0 and Γ_f are not colinear. The angle $\alpha \in [0, 2\pi)$ satisfies

$$\cos(\alpha) = \Gamma_0^\mathrm{T} \Gamma_f. \tag{14}$$

If Γ_0 and Γ_f are colinear, then these vectors are either equal or differ by a sign; if they are equal, then no attitude maneuver is required, whereas if they differ by a sign, then a is chosen to be an arbitrary direction perpendicular to Γ_0 with $\alpha = \pi$. A rest-to-rest attitude maneuver that meets the specified boundary conditions is

$$\begin{aligned} \Gamma(t) &= e^{a^\times \theta(t)} \Gamma_0 \\ &= [I + a^\times \sin\theta(t) + (a^\times)^2(1 - \cos\theta(t))]\Gamma_0, \qquad (15) \\ \omega(t) &= \dot\theta(t)a, \qquad (16) \\ u(t) &= \ddot\theta(t)Ja + \dot\theta(t)^2(a \times Ja), \qquad (17) \end{aligned}$$

where the rotation angle $\theta{:}[0, T] \to \mathbb{S}^1$ satisfies (12) and (13).

To achieve a full-attitude maneuver or a reduced-attitude maneuver that is not rest to rest, one possible approach is to select a sequence of three successive rotations. The first phase is based on selecting a fixed-axis rotation (with the rotation axis fixed in both the inertial and body frames) that brings the initial angular velocity of the rigid body to rest. The third phase is based on selecting a similar fixed-axis rotation that, in reverse time, brings the terminal angular velocity of the rigid body to rest. The second phase uses the framework presented in (8)–(13) and (14)–(17) to construct the rest-to-rest maneuver that transfers the attitude at the end of phase one to the required attitude at the beginning of phase three.

The framework presented in (8)–(13) and (14)–(17) can form the basis for planning attitude maneuvers. For example, $\theta(t)$ in (9)–(13) and (15)–(17) can be viewed as depending on parameter values that can be adjusted to achieve some attitude maneuver objective such as minimum time or minimum integrated norm of the control input using optimization algorithms. The key is the parameterization of attitude maneuvers in a form that satisfies the boundary conditions.

Observations on Controllability

The constructions given above demonstrate that the fully actuated rigid body is controllable even over arbitrarily

Attitude Set Notation

The following set-theoretic notation is used throughout this article.

- $\|x\|$ is the Euclidean norm of x.
- $\mathbb{S}^1 = \{(x_1, x_2) \in \mathbb{R}^2 \colon \|(x_1, x_2)\| = 1\}$ is the unit circle.
- $\mathbb{S}^2 = \{(x_1, x_2, x_3) \in \mathbb{R}^3 \colon \|(x_1, x_2, x_3)\| = 1\}$ is the two-sphere.
- $\mathbb{S}^3 = \{(x_1, x_2, x_3, x_4) \in \mathbb{R}^4 \colon \|(x_1, x_2, x_3, x_4)\| = 1\}$ is the three-sphere.
- $\mathrm{SO}(3) = \{R \in \mathbb{R}^{3\times 3} \colon RR^\mathrm{T} = R^\mathrm{T}R = I,\ \det(R) = 1\}$ is the special orthogonal group.
- $\mathfrak{so}(3) = \{U \in \mathbb{R}^{3\times 3} \colon U^\mathrm{T} = -U\}$ is the space of 3×3 skew-symmetric matrices, also the Lie algebra of $\mathrm{SO}(3)$.

The Impossibility of Global Attitude Stabilization Using Continuous Time-Invariant Feedback

The impossibility of global attitude stabilization using continuous time-invariant feedback is illustrated for planar rotations. The insight obtained for the case of attitude configurations on the unit circle $\mathbb{S}^1$ is helpful for understanding the analogous results when the attitude configurations are in $SO(3)$ or $\mathbb{S}^2$. Consider the attitude stabilization of the arm of the clock needle shown in Figure S3. We desire to stabilize the needle to the configuration in $\mathbb{S}^1$ indicated by point A by applying a force at the tip of the needle, which is tangent to the circle. Typical initial configurations are indicated by points B, C, or D. Each configuration can be moved to configuration A by either a clockwise force or a counterclockwise force, with the tip of the needle defining trajectories in $\mathbb{S}^1$ as shown in Figure S3. This explicit construction of forces indicates controllability. However, if we attempt to construct a continuous force vector field that rotates the needle to configuration A from each configuration or point on the circle, then an additional equilibrium (B) is born. This equilibrium (B) is created because on the upper half and lower half of the circle, the force vector fields are nonvanishing and point in opposing directions (either clockwise or counterclockwise) toward A. Since the force vector field is continuous, it must vanish at some point B, thereby creating a second equilibrium in addition to A.

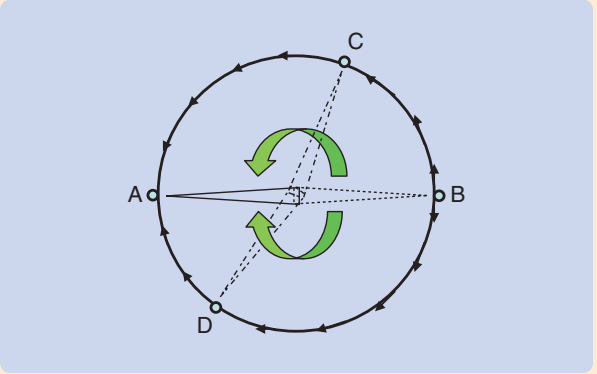

FIGURE S3 Illustration of the impossibility of global stabilization for planar rotations. In this case, the configuration manifold is the circle $\mathbb{S}^1$. To stabilize configuration A, a continuous force vector field that rotates the needle to configuration A from each configuration or point on the circle is constructed as shown by the vectors tangential to the circle. However, since this vector field points in the opposite direction in the upper half and lower half of the circle, the force vector field must vanish at some point B. The vanishing of the vector field at B creates a second equilibrium in addition to A. In a similar fashion, continuous time-invariant closed-loop vector fields yield multiple closed-loop equilibria on $SO(3)$ and $\mathbb{S}^2$.

short maneuver times. This observation is true for both full-attitude maneuvers and reduced-attitude maneuvers, thereby providing explicit constructions that demonstrate controllability.

We now show that the constructed maneuvers (8)–(13) and (14)–(17) are not continuous functions of the boundary conditions. For example, consider a reduced-attitude maneuver where Γ_0 and Γ_f lie along the north and south pole of $\mathbb{S}^2$, respectively. In this case, it follows from (12) and (13) that a slight perturbation in the initial condition can result in a control maneuver where the reduced attitude evolves through either the west or the east hemisphere of $\mathbb{S}^2$ depending on the perturbation. An analogous phenomenon occurs for attitude maneuvers on $SO(3)$. Thus, minor changes in the values of the initial attitude, initial angular velocity, terminal attitude, and terminal angular velocity may result in major changes in the attitude maneuver. This discontinuity is not due to the particular approach used for designing open-loop controllers. Rather, this discontinuity is a consequence of the non-Euclidean geometry of the special orthogonal group $SO(3)$ and the two-sphere $\mathbb{S}^2$.

GLOBAL ATTITUDE STABILIZATION

We now study fully actuated attitude stabilization and present results for both full- and reduced-attitude stabilization. The objective in full-attitude stabilization is to select a feedback control function

$$u : SO(3) \times \mathbb{R}^3 \to \mathbb{R}^3 \tag{18}$$

that asymptotically stabilizes a desired rigid body attitude equilibrium, while the objective in reduced-attitude stabilization is to select a feedback control function

$$u : \mathbb{S}^2 \times \mathbb{R}^3 \to \mathbb{R}^3 \tag{19}$$

that asymptotically stabilizes a desired rigid body reduced-attitude equilibrium. The desired attitude equilibrium or the reduced-attitude equilibrium is assumed to be specified, and the desired angular velocity vector is zero.

Since we assume full actuation, linear control theory can be applied to the linearization of the rigid-body equations of motion around a desired equilibrium to achieve local asymptotic stabilization. However, no continuous time-invariant feedback controller can globally asymptotically stabilize an equilibrium attitude of a rigid body [9], [16]; see "The Impossibility of Global Attitude Stabilization Using Continuous Time-Invariant Feedback." In fact, if we construct a continuous time-invariant feedback controller that locally asymptotically stabilizes a desired attitude equilibrium on $SO(3) \times \mathbb{R}^3$ or $\mathbb{S}^2 \times \mathbb{R}^3$, then the resulting closed-loop vector field must have more than one equilibrium.

Since no continuous time-invariant feedback controller can globally asymptotically stabilize a desired attitude equilibrium, we are faced with the following questions:

1) Since global asymptotic attitude stabilization using a continuous time-invariant feedback controller is impossible, can we obtain closed-loop stabilization properties that are nearly global?
2) What are the global properties of the resulting closed-loop system for a continuous time-invariant feedback controller?
3) Are there closed-loop performance implications for a continuous time-invariant feedback controller?

FULL-ATTITUDE STABILIZATION

We now present a proportional and derivative feedback control structure and characterize the resulting closed-loop vector field. We use this example to answer the above questions. We consider rigid-body attitude stabilization using the fully actuated rigid-body equations of motion

$$J\dot{\omega} = J\omega \times \omega + u, \tag{20}$$

$$\dot{R} = R\omega^{\times}, \tag{21}$$

where $R \in \mathrm{SO}(3)$ and $\omega \in \mathbb{R}^3$.

The *full-attitude stabilization* objective is to select a continuous feedback controller $u : \mathrm{SO}(3) \times \mathbb{R}^3 \to \mathbb{R}^3$ that asymptotically stabilizes the desired attitude equilibrium given by the desired attitude $R_{\mathrm{d}} \in \mathrm{SO}(3)$ and the angular velocity $\omega = 0$. The feedback controller is given by

$$u = -K_v\omega - K_p\Omega_{\mathbf{a}}(R), \tag{22}$$

where $K_v, K_p \in \mathbb{R}^{3\times 3}$ are positive definite matrices, $\mathbf{a} = [a_1 \ a_2 \ a_3]^{\top}$, where a_1, a_2, and a_3 are distinct positive integers, and the map

$$\Omega_{\mathbf{a}}(R) \triangleq \sum_{i=1}^{3} a_i e_i \times (R_{\mathrm{d}}^{\top} R e_i), \tag{23}$$

with $[e_1 \ e_2 \ e_3]$ the identity matrix. The feedback controller (22) requires the full attitude $R \in \mathrm{SO}(3)$ and angular velocity $\omega \in \mathbb{R}^3$, and it is continuous on $\mathrm{SO}(3) \times \mathbb{R}^3$. The feedback controller (22) can be interpreted as introducing a potential though the attitude-dependent term and dissipation through the angular-velocity-dependent term. Knowledge of the rigid-body inertia is not required by the feedback controller. While the dissipation term and the attitude-dependent term in the feedback controller appear linearly, the feedback controller is nonlinear since the rotation matrices are not elements of a vector space.

The closed-loop full-attitude dynamics using the controller (22) are

$$J\dot{\omega} = J\omega \times \omega - K_v\omega - K_p\Omega_{\mathbf{a}}(R), \tag{24}$$

$$\dot{R} = R\omega^{\times}. \tag{25}$$

Closed-Loop Equilibria

Let $(R_{\mathrm{e}}, \omega_{\mathrm{e}})$ be an equilibrium of the closed-loop system (24)–(25). Equating the right-hand side of (25) to zero yields $R_{\mathrm{e}}\omega_{\mathrm{e}}^{\times} = 0$. Since R_{e} is invertible, we obtain $\omega_{\mathrm{e}} = 0$. Substituting $\omega_{\mathrm{e}} = 0$ in (24) and equating it to zero yields $\Omega_{\mathbf{a}}(R_{\mathrm{e}}) = 0$. It can be shown [23] that there are four closed-loop equilibria that satisfy $\Omega_{\mathbf{a}}(R_{\mathrm{e}}) = 0$ and $\omega_{\mathrm{e}} = 0$.

Proposition 1

$(R_{\mathrm{e}}, 0)$ is an equilibrium of the closed-loop attitude equations of motion (24)–(25) if and only if

$$R_{\mathrm{d}}^{\top} R_{\mathrm{e}} \in \mathcal{S} \triangleq \{[e_1 \ e_2 \ e_3], [e_1 \ -e_2 \ -e_3], [-e_1 \ -e_2 \ e_3], [-e_1 \ e_2 \ -e_3]\}. \tag{26}$$

That is, $(R_{\mathrm{e}}, 0) \in \mathcal{E}$, where

$$\mathcal{E} \triangleq \{(R_{\mathrm{d}}, 0), (R_{\alpha}, 0), (R_{\beta}, 0), (R_{\gamma}, 0)\}, \tag{27}$$

where

$$R_{\alpha} \triangleq R_{\mathrm{d}}[e_1 \quad -e_2 \quad -e_3], \tag{28}$$

$$R_{\beta} \triangleq R_{\mathrm{d}}[-e_1 \ -e_2 \quad e_3], \tag{29}$$

$$R_{\gamma} \triangleq R_{\mathrm{d}}[-e_1 \quad e_2 \quad -e_3]. \tag{30}$$

Proof

Equating $\Omega_{\mathbf{a}}(R_{\mathrm{e}}) = 0$ yields

$$a_1 e_1 \times R_{\mathrm{d}}^{\top} R_{\mathrm{e}} e_1 + a_2 e_2 \times R_{\mathrm{d}}^{\top} R_{\mathrm{e}} e_2 + a_3 e_3 \times R_{\mathrm{d}}^{\top} R_{\mathrm{e}} e_3 = 0. \tag{31}$$

Writing $R_{\mathrm{d}}^{\top} R_{\mathrm{e}} = [r_{i,j}]_{i,j\in\{1,2,3\}} \in \mathrm{SO}(3)$ and expanding the cross products, (31) is equivalent to $a_2 r_{32} = a_3 r_{23}$, $a_1 r_{31} = a_3 r_{13}$, $a_1 r_{21} = a_2 r_{12}$. Since a_1, a_2, and a_3 are positive, the rotation matrix $R_{\mathrm{d}}^{\top} R_{\mathrm{e}}$ can be written as

$$R_{\mathrm{d}}^{\top} R_{\mathrm{e}} = \begin{bmatrix} r_{11} & r_{12} & r_{13} \\ \frac{a_2}{a_1} r_{12} & r_{22} & r_{23} \\ \frac{a_3}{a_1} r_{13} & \frac{a_3}{a_2} r_{23} & r_{33} \end{bmatrix}. \tag{32}$$

Since $R_{\mathrm{d}}^{\top} R_{\mathrm{e}}$ is orthogonal it follows that

$$\left(1 - \frac{a_2^2}{a_1^2}\right) r_{12}^2 + \left(1 - \frac{a_3^2}{a_1^2}\right) r_{13}^2 = 0, \tag{33}$$

$$\left(1 - \frac{a_3^2}{a_1^2}\right) r_{13}^2 + \left(1 - \frac{a_3^2}{a_2^2}\right) r_{23}^2 = 0, \tag{34}$$

$$\left(1 - \frac{a_2^2}{a_1^2}\right) r_{12}^2 - \left(1 - \frac{a_3^2}{a_2^2}\right) r_{23}^2 = 0. \tag{35}$$

Since a_1, a_2, and a_3 are distinct, the solution to (33)–(35) satisfies either a) $r_{12} = r_{13} = r_{23} = 0$ or b) none of the r_{ij}, $i \neq j$ are zero. To see this result, first note that a) is a trivial solution of (33)–(35). Suppose $r_{12} \neq 0$. Then since a_1, a_2, and a_3 are distinct, it follows that $(1 - (a_2^2/a_1^2)) \neq 0$, $(1 - (a_3^2/a_1^2)) \neq 0$, and $(1 - (a_3^2/a_2^2)) \neq 0$. Then, since $r_{12} \neq 0$, (33) yields that $r_{13} \neq 0$, and from (34), it follows that $r_{23} \neq 0$. Similar arguments hold for the case $r_{13} \neq 0$ and $r_{23} \neq 0$. Thus, every solution to (33)–(35) satisfies either a) or b).

Next, consider case b). Suppose $a_1 > a_2$. Then, $(1 - (a_2^2/a_1^2))r_{12}^2 > 0$ since $r_{12} \neq 0$, and hence (33) yields $(1 - (a_3^2/a_1^2))r_{13}^2 < 0$. Since r_{13}^2 is positive, it follows that $a_3 > a_1$. Thus, $a_3 > a_1 > a_2$. This inequality implies

$$\left(1 - \frac{a_3^2}{a_1^2}\right)r_{13}^2 < 0, \quad \left(1 - \frac{a_3^2}{a_2^2}\right)r_{23}^2 < 0.$$

Therefore, the left-hand side of (34) is negative, yielding a contradiction. Similar arguments show that for $a_1 < a_2$, (33)–(35) yields a contradiction for case b). Hence since a_1, a_2, and a_3 are distinct, case b) yields a contradiction, and the only solution to (33)–(35) is case a), that is, $r_{12} = r_{13} = r_{23} = 0$.

Then, substituting $r_{12} = r_{13} = r_{23} = 0$ into (32), it follows that r_{11}, r_{22}, r_{33} each have value $+1$ or -1. Thus, $R_{\mathrm{d}}^{\mathrm{T}} R_{\mathrm{e}} \in \mathcal{S}$ as given in (26), and hence $(R_{\mathrm{e}}, 0) \in \mathcal{E}$ in (27). □

Proposition 1 shows that the continuous feedback controller results in a closed-loop system with four distinct equilibria. One of these equilibria is the desired equilibrium specified by the attitude R_{d}, while the remaining equilibria are designated by R_α, R_β, and R_γ. These attitudes differ from the desired attitude R_{d} by 180° of rotation about each of the three body-fixed axes.

Local Structure of the Closed-Loop System

We next analyze the stability of the desired equilibrium and each of the three additional equilibria, and we deduce the local structure of the closed-loop vector field near each of these equilibria using the Lie group properties of SO(3). Since $\dim[\mathrm{SO}(3) \times \mathbb{R}^3] = 6$, each linearization evolves on $\mathbb{R}^6$. To obtain the local structure of the closed-loop attitude dynamics, we linearize the closed-loop equations about each equilibrium. While it is possible to study the linearized dynamics in local coordinates, the closed-loop vector field (24)–(25) can also be linearized using the Lie-group properties of the non-Euclidean manifold SO(3). Let $(R_{\mathrm{e}}, 0) \in \mathcal{E}$ be an equilibrium solution of the closed-loop system (24)–(25). Consider a perturbation of the equilibrium $(R_{\mathrm{e}}, 0) \in \mathcal{E}$ in terms of a perturbation parameter $\varepsilon \in \mathbb{R}$. We can express the perturbation as a rotation matrix in SO(3) using exponential coordinates [34]–[37]. This representation guarantees that the perturbation is a rotation matrix for all values of the perturbation parameter.

Let the perturbation in the initial attitude be given as $R(0, \varepsilon) = R_{\mathrm{e}} e^{\varepsilon \Theta_0^{\times}}$, where $R_{\mathrm{d}}^{\mathrm{T}} R_{\mathrm{e}} \in \mathcal{S}$ is given in (26) and $\Theta_0 \in \mathbb{R}^3$; see "Linearization of Nonlinear Models on Euclidean Spaces and Non-Euclidean Spaces" for details. The perturbation in the initial angular velocity is given as $\omega(0, \varepsilon) = \varepsilon\omega_0$, where $\omega_0 \in \mathbb{R}^3$. Note that if $\varepsilon = 0$ then $(R(0, 0), \omega(0, 0)) = (R_{\mathrm{e}}, 0)$, and hence

$$(R(t, 0), \omega(t, 0)) \equiv (R_{\mathrm{e}}, 0) \tag{36}$$

for all time $t \in [0, \infty)$, thereby obtaining the equilibrium solution.

Next, consider the solution to the perturbed equations of motion for the closed-loop system (24)–(25). These equations are given by

$$J\dot{\omega}(t, \varepsilon) = J\omega(t, \varepsilon) \times \omega(t, \varepsilon) - K_v\omega(t, \varepsilon) - K_p\Omega_{\mathbf{a}}(R(t, \varepsilon)), \tag{37}$$

$$\dot{R}(t, \varepsilon) = R(t, \varepsilon)\omega(t, \varepsilon)^{\times}. \tag{38}$$

To linearize (24)–(25), we differentiate both sides of (37) and (38) with respect to ε and substitute $\varepsilon = 0$, yielding

$$J\dot{\omega}_\varepsilon(t, 0) = -K_v\omega_\varepsilon(t, 0) - K_p\Omega_{\mathbf{a}}(R_\varepsilon(t, 0)), \tag{39}$$

$$\dot{R}_\varepsilon(t, 0) = R_{\mathrm{e}}\omega_\varepsilon(t, 0)^{\times}, \tag{40}$$

where $\omega_\varepsilon(t, 0) \triangleq (\partial\omega(t, \varepsilon)/(\partial\varepsilon))_{\varepsilon=0}$ and $R_\varepsilon(t, 0) \triangleq (\partial R(t, \varepsilon)/(\partial\varepsilon))_{\varepsilon=0}$. Now we define the linearized states $\Delta\omega, \Delta\Theta \in \mathbb{R}^3$ as $\Delta\omega(t) \triangleq \omega_\varepsilon(t, 0)$ and $\Delta\Theta(t)^{\times} \triangleq R_{\mathrm{e}}^{\mathrm{T}} R_\varepsilon(t, 0)$. Then from (40) we obtain

$$\Delta\dot{\Theta}(t)^{\times} = R_{\mathrm{e}}^{\mathrm{T}}\dot{R}_\varepsilon(t, 0) = \omega_\varepsilon(t, 0)^{\times} = \Delta\omega(t)^{\times}.$$

Suppressing the time dependence, we obtain

$$\Delta\dot{\Theta} = \Delta\omega. \tag{41}$$

From (39), we obtain

$$J\Delta\dot{\omega} = -K_v\Delta\omega - K_p\Omega_{\mathbf{a}}(R_{\mathrm{e}}\Delta\Theta^{\times}). \tag{42}$$

Now,

$$\begin{aligned}\Omega_{\mathbf{a}}(R_{\mathrm{e}}\Delta\Theta^{\times}) &= a_1e_1 \times (R_{\mathrm{d}}^{\mathrm{T}}R_{\mathrm{e}}\Delta\Theta^{\times}e_1) + a_2e_2 \times (R_{\mathrm{d}}^{\mathrm{T}}R_{\mathrm{e}}\Delta\Theta^{\times}e_2)\\ &\quad + a_3e_3 \times (R_{\mathrm{d}}^{\mathrm{T}}R_{\mathrm{e}}\Delta\Theta^{\times}e_3),\\ &= -(a_1e_1^{\times}R_{\mathrm{d}}^{\mathrm{T}}R_{\mathrm{e}}e_1^{\times} + a_2e_2^{\times}R_{\mathrm{d}}^{\mathrm{T}}R_{\mathrm{e}}e_2^{\times}\\ &\quad + a_3e_3^{\times}R_{\mathrm{d}}^{\mathrm{T}}R_{\mathrm{e}}e_3^{\times})\Delta\Theta,\end{aligned} \tag{43}$$

where $R_{\mathrm{d}}^{\mathrm{T}}R_{\mathrm{e}}$ belongs to $\mathcal{S}$ as given in (26) in Proposition 1.

Combining (41)–(43), we obtain the linearization of the closed-loop system (24)–(25) about each equilibrium in (27) as

$$J\Delta\ddot{\Theta} + K_v\Delta\dot{\Theta} + \mathsf{K}\Delta\Theta = 0, \tag{44}$$

Linearization of Nonlinear Models on Euclidean Spaces and Non-Euclidean Spaces

Linearization of a nonlinear model is defined from the responses to an infinitesimal perturbation of initial conditions from a given equilibrium. For rigid-body rotational dynamics, we require that the perturbations in initial conditions lie on the manifold $SO(3) \times \mathbb{R}^3$ so that the solution evolves on the manifold $SO(3) \times \mathbb{R}^3$.

Let $\mathcal{F}: SO(3) \times \mathbb{R}^3 \times \mathbb{R} \to SO(3) \times \mathbb{R}^3$ be the mapping such that $\mathcal{F}(R_e, \omega_e, \varepsilon)$ represents the perturbation from the equilibrium (R_e, ω_e), where ε denotes the perturbation parameter. Thus $\varepsilon = 0$ implies no perturbation from the equilibrium solution. If $(R(t, \varepsilon), \omega(t, \varepsilon))$ represents the unique solution corresponding to the perturbation ε, then the linearization is obtained by differentiating this perturbed solution with respect to ε, where the perturbation function is defined as

$$\mathcal{F}(R_e, \omega_e, \varepsilon) \triangleq (R_e e^{\varepsilon \Theta_0^\times}, \omega_e + \varepsilon \omega_0) \tag{S1}$$

and $(\Theta_0, \omega_0) \in \mathbb{R}^3 \times \mathbb{R}^3$. This computation yields the linearization of the rigid-body rotational dynamics at the equilibrium. A similar analysis can be used to linearize the reduced rotational dynamics of a rigid body.

In contrast to the nonlinear perturbation function (S1) for rigid-body rotational dynamics, we can choose $\mathcal{F}$ as a linear additive vector perturbation for models whose states evolve on Euclidean spaces. For attitude dynamics, while a linear additive perturbation is used for the angular velocity, the exponential function is used for the attitude perturbation in (S1). The reason behind this choice is that, while linear additive perturbations guarantee that, for all values of the perturbation parameter ε, the resulting angular velocity perturbations lie in the Euclidean space of angular velocities, adding rotation matrices does not guarantee that the resulting matrix is also a rotation matrix. Since the exponential map (2) of $SO(3)$ guarantees that the resulting matrix is a rotation matrix [34], [14], [36], [37], an exponential function is used to construct the attitude perturbation as shown in (S1). Thus, the attitude perturbation in (S1) lies in $SO(3)$ for all values of the perturbation parameter ε.

where the constant matrix K, depending on the equilibrium attitude, is defined as

$$\mathsf{K} = \begin{cases} K_p \operatorname{diag}(a_2 + a_3, a_1 + a_3, a_1 + a_2), & \text{if } R_e = R_d, \\ -K_p \operatorname{diag}(a_2 + a_3, a_1 - a_3, a_1 - a_2), & \text{if } R_e = R_\alpha, \\ -K_p \operatorname{diag}(a_3 - a_2, a_3 - a_1, a_1 + a_2), & \text{if } R_e = R_\beta, \\ -K_p \operatorname{diag}(a_2 - a_3, a_1 + a_3, a_2 - a_1), & \text{if } R_e = R_\gamma. \end{cases} \tag{45}$$

Thus, the local attitude dynamics near each of the four equilibrium solutions are given by a linear second-order mechanical system with positive damping. The stiffness depends on the equilibrium; near the desired equilibrium, the stiffness is positive definite, and hence, the local attitude dynamics near the desired equilibrium are locally exponentially stable. Around the additional three equilibria corresponding to the attitudes R_α, R_β, and R_γ, the stiffness matrix has at least one negative eigenvalue resulting in a saddle point. Therefore, the closed-loop dynamics near each equilibrium solution are unstable. Furthermore, these equilibria have no zero eigenvalues, yielding the following result.

Proposition 2

The equilibrium $(R_d, 0)$ of the closed-loop equations (24)–(25) is asymptotically stable with locally exponential convergence. The additional closed-loop equilibria $(R_\alpha, 0)$, $(R_\beta, 0)$, and $(R_\gamma, 0)$ are hyperbolic and unstable.

Global Analysis of the Full-Attitude Closed-Loop System

The feedback controller (22) renders the desired equilibrium $(R_d, 0)$ locally asymptotically stable with local exponential convergence. Since the feedback controller is continuous, the closed-loop vector field has the additional equilibria $(R_\alpha, 0)$, $(R_\beta, 0)$, and $(R_\gamma, 0)$.

We next want to understand the global structure of the solutions of the closed-loop system. Consider again the closed-loop linearizations (44). For each linearization about the unstable equilibria $(R_\alpha, 0)$, $(R_\beta, 0)$, and $(R_\gamma, 0)$, the linearization has at least one eigenvalue with a negative real part and at least one eigenvalue with a positive real part. Furthermore, the four equilibria are hyperbolic, that is, the linearization has no imaginary eigenvalues. Thus, local properties of the closed-loop vector field near each of these equilibria are as follows. There exist stable and unstable manifolds for each of the equilibria $(R_\alpha, 0)$, $(R_\beta, 0)$, and $(R_\gamma, 0)$, denoted by $(\mathcal{W}^s_\alpha, \mathcal{W}^u_\alpha)$, $(\mathcal{W}^s_\beta, \mathcal{W}^u_\beta)$, and $(\mathcal{W}^s_\gamma, \mathcal{W}^u_\gamma)$ such that all solutions that start on the stable manifold converge to the corresponding unstable equilibrium, and all solutions that start on the unstable manifold locally diverge from the corresponding equilibrium [38]. Furthermore, the dimensions of the stable and unstable manifolds of each unstable equilibrium are the same as the number of eigenvalues with negative and positive real parts, respectively [38].

Since the union of the stable manifolds has dimension less than six, it can be shown [23] that the set has measure zero and is nowhere dense. Furthermore, using Lyapunov analysis [23], it can be shown that all solutions converge to one of the four equilibria. Since all solutions that converge to the three unstable equilibria lie in a nowhere dense set, almost all closed-loop solutions converge to the desired equilibrium $(R_d, 0)$. This result is precisely stated in the following theorem.

Theorem 1

Consider the closed-loop rigid-body attitude equations of motion given by (24) and (25) for the controller (22), where K_p and K_v are positive definite, and a_1, a_2, and a_3 are distinct positive integers. Then the closed-loop equilibrium $(R_{\mathrm{d}}, 0)$ is asymptotically stable with locally exponential convergence. Furthermore, there exists a nowhere dense set $\mathcal{M}$ such that all solutions starting in $\mathcal{M}$ converge to one of the unstable equilibria $(R_\alpha, 0)$, $(R_\beta, 0)$, and $(R_\gamma, 0)$, and all remaining solutions converge to the desired equilibrium $(R_{\mathrm{d}}, 0)$. Thus, the domain of attraction of the desired equilibrium $(R_{\mathrm{d}}, 0)$ is almost global.

Since the domain of attraction of $(R_{\mathrm{d}}, 0)$ is the complement of the union of the stable manifolds for each of the three unstable equilibria, the eigenspace corresponding to the stable eigenvalues of an unstable equilibrium provides explicit local information on the complement of the domain of attraction of $(R_{\mathrm{d}}, 0)$ near that unstable equilibrium. Note that the structure and characteristic of the unstable equilibria depends on the particular choice of feedback control. However, as shown in [9], the complement of the domain of attraction of $(R_{\mathrm{d}}, 0)$ is necessarily nonempty for every continuous time-invariant feedback controller on $\mathrm{SO}(3) \times \mathbb{R}^3$. Thus, the existence of a nowhere dense set, which is the complement of the domain of attraction of $(R_{\mathrm{d}}, 0)$, is not a consequence of the specific controller (22). Since global stabilization using continuous time-invariant feedback is impossible, almost global stabilization is the best possible result for this stabilization problem.

REDUCED-ATTITUDE STABILIZATION

Rigid-body reduced-attitude stabilization is analyzed using the fully actuated rigid-body equations of motion

$$J\dot{\omega} = J\omega \times \omega + u, \tag{46}$$

$$\dot{\Gamma} = \Gamma \times \omega, \tag{47}$$

where $\Gamma \in \mathbb{S}^2$ and $\omega \in \mathbb{R}^3$.

The objective of *reduced-attitude stabilization* is to select a continuous feedback controller $u : \mathbb{S}^2 \times \mathbb{R}^3 \to \mathbb{R}^3$ that asymptotically stabilizes the desired reduced-attitude equilibrium defined by the reduced-attitude vector $\Gamma_{\mathrm{d}} \in \mathbb{S}^2$ and angular velocity vector $\omega = 0$. The feedback controller is given by

$$u = k_p(\Gamma_{\mathrm{d}} \times \Gamma) - K_v\omega, \tag{48}$$

where k_p is a positive real number and K_v is a positive definite matrix. This feedback controller is based on feedback of the reduced attitude $\Gamma = R^{\mathrm{T}}b \in \mathbb{S}^2$ and the angular velocity $\omega \in \mathbb{R}^3$, and it is continuous on $\mathbb{S}^2 \times \mathbb{R}^3$. The feedback controller (48) can be interpreted as introducing a potential through the reduced-attitude-dependent term and dissipation through the angular velocity-dependent term. Knowledge of the rigid-body inertia is not required by the feedback controller. Note that while the dissipation term and the reduced-attitude-dependent term in the feedback controller appear linearly, the feedback controller is nonlinear since the reduced-attitude vectors lie in $\mathbb{S}^2$ and, hence, are not elements of a vector space.

The closed-loop reduced-attitude equations of motion are

$$J\dot{\omega} = J\omega \times \omega + k_p(\Gamma_{\mathrm{d}} \times \Gamma) - K_v\omega, \tag{49}$$

$$\dot{\Gamma} = \Gamma \times \omega. \tag{50}$$

Closed-Loop Equilibria

Consider the equilibrium structure of the closed-loop equations (49) and (50). Equating the right-hand side of (49) and (50) to zero yields that an equilibrium at $(\Gamma_{\mathrm{e}}, \omega_{\mathrm{e}})$ satisfies $\omega_{\mathrm{e}} = \mu\Gamma_{\mathrm{e}}$, where μ is a constant, and

$$\mu^2 J\Gamma_{\mathrm{e}} \times \Gamma_{\mathrm{e}} + k_p(\Gamma_{\mathrm{d}} \times \Gamma_{\mathrm{e}}) - \mu K_v\Gamma_{\mathrm{e}} = 0.$$

Premultiplying both sides by $\Gamma_{\mathrm{e}}^{\mathrm{T}}$ yields $\mu\Gamma_{\mathrm{e}}^{\mathrm{T}}K_v\Gamma_{\mathrm{e}} = 0$. Since K_v is positive definite and $\|\Gamma_{\mathrm{e}}\| = 1$, it follows that $\mu = 0$. Thus, $\omega_{\mathrm{e}} = 0$. Then, we see that $\Gamma_{\mathrm{e}} \times \Gamma_{\mathrm{d}} = 0$, and hence $\Gamma_{\mathrm{e}} = \pm\Gamma_{\mathrm{d}}$. We thus have the following proposition.

Proposition 3

The reduced closed-loop attitude equations of motion (49) and (50) have two equilibrium solutions given by $(\Gamma_{\mathrm{d}}, 0)$ and $(-\Gamma_{\mathrm{d}}, 0)$.

Proposition 3 shows that the continuous time-invariant feedback control results in a closed-loop system with two distinct equilibria given by the desired equilibrium $(\Gamma_{\mathrm{d}}, 0)$ and an additional closed-loop equilibrium $(-\Gamma_{\mathrm{d}}, 0)$. The existence of the two reduced-attitude equilibria implies that there is a manifold of full-attitude equilibria, all of which satisfy $R^{\mathrm{T}}b = \Gamma_{\mathrm{d}}$, and another disjoint manifold of full-attitude equilibria, all of which satisfy $R^{\mathrm{T}}b = -\Gamma_{\mathrm{d}}$; see "Relation Between Full Attitude and Reduced Attitude."

Local Structure of the Closed-Loop System

We study linearizations of the closed-loop equations (49) and (50) about the equilibrium $(\Gamma_{\mathrm{d}}, 0)$ and about the equilibrium $(-\Gamma_{\mathrm{d}}, 0)$. Since $\dim[\mathbb{S}^2 \times \mathbb{R}^3] = 5$, each linearization evolves on $\mathbb{R}^5$. Similar to the analysis presented in [23], it can be shown that each equilibrium solution has the following local properties.

Proposition 4

The equilibrium $(\Gamma_{\mathrm{d}}, 0)$ of the closed-loop reduced-attitude equations (49) and (50) is asymptotically stable and the convergence is locally exponential. Furthermore, the equilibrium $(-\Gamma_{\mathrm{d}}, 0)$ is hyperbolic and unstable.

Global Analysis of the Reduced-Attitude Closed-Loop System

In this section, we study the global behavior of the closed-loop system defined by (49) and (50). The results are parallel to those stated above for the full-attitude closed-loop system. In particular, we characterize the domain of attraction of the desired equilibrium $(\Gamma_d, 0)$ and describe the global structure of the solutions that converge to the unstable equilibrium $(-\Gamma_d, 0)$.

It can be shown using Lyapunov analysis that all closed-loop solutions converge to one of the two closed-loop equilibria (see "Lyapunov Analysis on $SO(3) \times \mathbb{R}^3$ and $\mathbb{S}^2 \times \mathbb{R}^3$"). Since $(-\Gamma_d, 0)$ is unstable and the linearization about $(-\Gamma_d, 0)$ has no imaginary or zero eigenvalues, it follows that there exists a stable invariant manifold $\mathcal{M}_r$ [38] of the closed-loop equations (49) and (50) such that all solutions that start in $\mathcal{M}_r$ converge to $(-\Gamma_d, 0)$. The tangent space to this manifold at $(-\Gamma_d, 0)$ is the stable eigenspace corresponding to the negative eigenvalues. Since the linearization of the closed-loop dynamics at $(-\Gamma_d, 0)$ has no eigenvalues on the imaginary axis, the closed-loop dynamics has no center manifold, and every closed-loop solution that converges to $(-\Gamma_d, 0)$ lies in the stable manifold $\mathcal{M}_r$.

It can be shown that $\mathcal{M}_r$ is a lower dimensional subset in the five-dimensional manifold $\mathbb{S}^2 \times \mathbb{R}^3$ and is nowhere dense [23]. Hence, the closed-loop dynamics partition $\mathbb{S}^2 \times \mathbb{R}^3$ into two sets. The first set $\mathcal{M}_r$ is defined by solutions that converge to the unstable equilibrium $(-\Gamma_d, 0)$, and its complement is defined by the dense set of all solutions that converge to the desired equilibrium $(\Gamma_d, 0)$. Thus, $(\Gamma_d, 0)$ is an asymptotically stable equilibrium of the closed-loop system (49) and (50) with an almost global domain of attraction.

Theorem 2

Consider the reduced rigid-body attitude dynamics given by the closed-loop equations (49) and (50). Assume that k_p is positive, and K_v is symmetric and positive definite. Then the closed-loop equilibrium $(\Gamma_d, 0)$ is asymptotically stable with local exponential convergence. Furthermore, there exists a lower dimensional manifold $\mathcal{M}_r$ that is nowhere dense such that closed-loop solutions starting in $\mathcal{M}_r$ converge to the unstable equilibrium $(-\Gamma_d, 0)$ and all remaining closed-loop solutions converge to the desired equilibrium $(\Gamma_d, 0)$. Thus, the domain of attraction of the desired equilibrium is almost global.

Since the domain of attraction of $(\Gamma_d, 0)$ is the complement of the stable manifold of the unstable equilibrium $(-\Gamma_d, 0)$, the eigenspace corresponding to the stable eigenvalues of $(-\Gamma_d, 0)$ provides explicit local information on the complement of the domain of attraction of $(\Gamma_d, 0)$ near $(-\Gamma_d, 0)$. The presence of the nowhere dense set, which is the complement of the domain of attraction of $(\Gamma_d, 0)$, is not a consequence of the specific controller that is studied in this article. Rather, the complement of the domain of attraction of $(\Gamma_d, 0)$ is necessarily nonempty for every continuous time-invariant feedback controller on $\mathbb{S}^2 \times \mathbb{R}^3$ [9]. Thus, since global stabilization using continuous time-invariant feedback is impossible, almost global stabilization is the best possible result for this stabilization problem.

Relation Between Full Attitude and Reduced Attitude

For a rigid body, one reduced attitude corresponds to a manifold of full attitudes. To see this connection, note that the definition of the reduced attitude $\Gamma \in \mathbb{S}^2$ implies that there exists a full attitude $R_0 \in SO(3)$ such that $R_0^T b = \Gamma$. Then Rodrigues's formula shows that every full attitude given by $R = R_0 \exp(\alpha \Gamma^\times)$ with $\alpha \in \mathbb{R}$ also satisfies $R^T b = \Gamma$. In physical terms, all full attitudes that differ by a rotation about Γ are equivalent in the sense that they have the same reduced attitude, namely, Γ.

CLOSED-LOOP PERFORMANCE LIMITATIONS

The difference between global asymptotic stability and almost global asymptotic stability of the desired equilibrium of a closed-loop attitude control system leads to certain closed-loop attitude performance limitations. Thus, we now address the third question posed in the section "Global Attitude Stabilization" related to performance implications of almost global stabilization.

While all solutions that lie in the domain of attraction asymptotically approach the desired equilibrium, solutions that encounter a sufficiently small neighborhood of the stable manifold of one of the unstable hyperbolic equilibria can remain near that stable manifold for an arbitrarily long

Lyapunov Analysis on $SO(3) \times \mathbb{R}^3$ and $\mathbb{S}^2 \times \mathbb{R}^3$

Closed-loop full-attitude dynamics evolve on the non-Euclidean manifold $SO(3) \times \mathbb{R}^3$, while closed-loop reduced-attitude dynamics evolve on the non-Euclidean manifold $\mathbb{S}^2 \times \mathbb{R}^3$. Since these manifolds are locally Euclidean, local stability properties of a closed-loop equilibrium solution can be assessed using standard Lyapunov methods. In addition, the LaSalle invariance result and related Lyapunov results apply to closed-loop vector fields defined on these manifolds. However, since the manifolds $SO(3)$ and $\mathbb{S}^2$ are compact, the radial unboundedness assumption cannot be satisfied; consequently, global asymptotic stability cannot follow from a Lyapunov analysis on Euclidean spaces [40], and therefore must be analyzed in alternative ways [19]–[23].

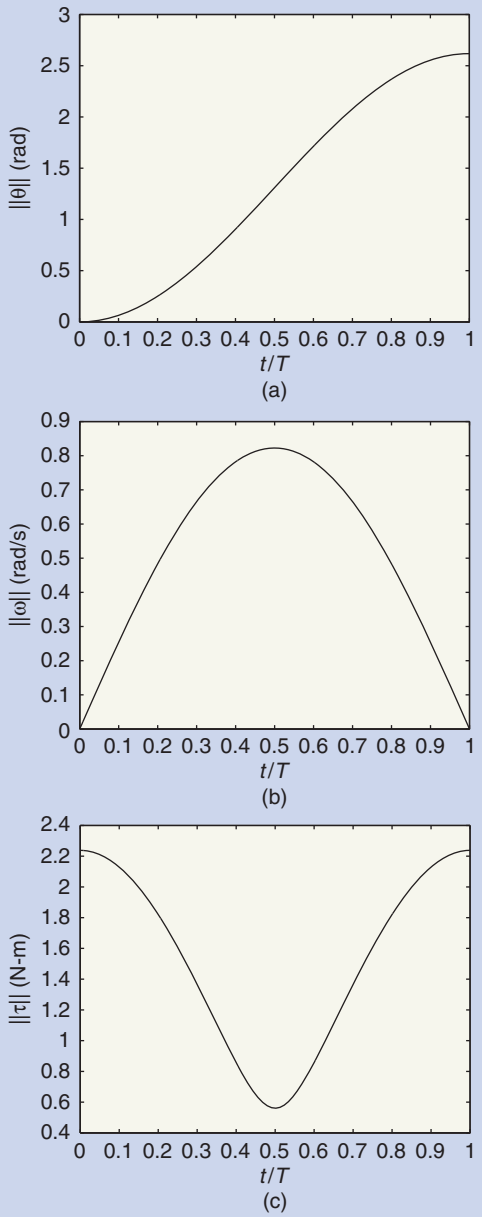

FIGURE 1 (a) Principal angle, (b) norm of angular velocity, and (c) norm of the control torque plotted versus normalized time for the rest-to-rest, full-attitude, open-loop maneuver for a rigid body with principal moment of inertia matrix $J = \text{diag}(3, 4, 5)$ kg-m^2 within the maneuver time $T = 5$ s. The principal angle $\theta(t)$ is obtained as a sinusoidal interpolation between the given initial attitude $R(0)$ and the desired final attitude $R(T)$ for this rest-to-rest maneuver. The angular velocity and control torque are obtained from the principal angle and resulting attitude profile.

period of time [38]. Such solutions in the domain of attraction approach the desired equilibrium arbitrarily slowly. This property of the closed-loop system is an attitude performance limitation that arises due to the inherent closed-loop properties of a continuous time-invariant vector field on $\text{SO}(3) \times \mathbb{R}^3$ or $\mathbb{S}^2 \times \mathbb{R}^3$.

In contrast to continuous feedback controllers, switched or discontinuous feedback controllers can also be considered for attitude control. Controllers based on nonsmooth feedback may not suffer from the performance limitations observed in smooth controllers [27]. However, discontinuous controllers suffer from chattering at the surface of the discontinuity of the closed-loop vector field. Chattering in discontinuous controllers can be resolved by using hysteresis [39]. However, this discontinuity can render standard Lyapunov theory inapplicable due to the non-Lipschitz nature of the closed-loop vector field [40], [41].

EXAMPLES OF RIGID-BODY ATTITUDE MANEUVERS AND ATTITUDE STABILIZATION

We now illustrate the attitude control results by constructing a rest-to-rest full-attitude maneuver, a rest-to-rest reduced-attitude maneuver, a full-attitude stabilizing feedback controller, and a reduced-attitude stabilizing feedback controller. The rigid body is assumed to be an asymmetric body. The body-fixed frame is defined by the principal axes of the body, and the body inertia matrix is assumed to be $J = \text{diag}(3, 4, 5)$ kg-m^2.

A Rest-to-Rest Full-Attitude Maneuver

We construct a rest-to-rest full-attitude maneuver that aligns the three principal axes of the rigid body with the three inertial axes. Specifically, the full-attitude maneuver transfers the initial attitude R_0 to a terminal attitude R_f, where

$$R_0 = \begin{bmatrix} -0.3995 & 0.8201 & 0.4097 \\ 0.1130 & -0.3995 & 0.9097 \\ 0.9097 & 0.4097 & 0.0670 \end{bmatrix}, \quad R_f = \begin{bmatrix} 1 & 0 & 0 \\ 0 & 1 & 0 \\ 0 & 0 & 1 \end{bmatrix},$$

in a maneuver time of $T = 5$ s. Equation (8) can be solved to obtain $a = (0.5, 0.5, 0.707)$, and the angle $\alpha = 5\pi/6$ rad. Expressions for the attitude, angular velocity, and control input that satisfy the specified boundary conditions are given by (9)–(11). In this instance, the rotation angle is $\theta(t) = (\alpha/2)(1 - \cos((\pi/T)t))$ rad.

For the rest-to-rest full-attitude maneuver, Figure 1 shows the time responses for the principal angle θ, the norm of the angular velocity $\|\omega\|$, and the norm of the control torque $\|u\|$ versus normalized time t/T. Numerical solutions for these open-loop maneuvers are obtained using Lie group variational integrators, as described in "Numerical Integration of Attitude Control Systems." With this control scheme and fixed initial and final attitudes, the normalized time plots for the principal angle, the angular velocity norm, and control norm for every final time T qualitatively look similar to those shown in Figure 1, except that larger T requires less control effort.

Numerical Integration of Attitude Control Systems

Equations (24) and (25) describe the full-attitude control system, whereas (49) and (50) describe the reduced-attitude control system, which evolve on $\mathrm{SO}(3) \times \mathbb{R}^3$ and on $\mathbb{S}^2 \times \mathbb{R}^3$, respectively. Traditional numerical integration schemes, developed for differential equations that evolve on $\mathbb{R}^n$, do not guarantee that the computed solution lies in the appropriate manifold [S1]. In contrast to traditional numerical integration schemes, geometrical numerical integration schemes guarantee that the computed solution lies in the appropriate manifold [S1]. Geometric integration schemes can be applied to manifolds such as $\mathbb{S}^3$ without requiring renormalization or projection. If the manifold under consideration is a Lie group such as $\mathrm{SO}(3)$, then such integration schemes are called Lie group methods. Integration methods that are obtained by using the discrete version of the variational principle of mechanics are called variational integrators. In [S2]–[S4], Lie group variational integrators are developed and used to numerically simulate attitude dynamics and control systems. Lie group variational integrators incorporate the desirable features of both geometric integration schemes and variational integration schemes.

REFERENCES

[S1] E. Hairer, C. Lubich, and G. Wanner, *Geometric Numerical Integration*. New York: Springer-Verlag, 2000.

[S2] T. Lee, M. Leok, and N. H. McClamroch, "Computational geometric optimal control of rigid bodies," *Commun. Inform. Syst.*, vol. 8, no. 4. pp. 435–462, 2008.

[S3] T. Lee, M. Leok, and N. H. McClamroch, "Lagrangian mechanics and variational integrators on two-spheres," *Int. J. Numerical Methods Eng.*, vol. 79, pp. 1147–1174, 2009.

[S4] A. K. Sanyal and N. Nordkvist, "A robust estimator for almost global attitude feedback tracking," in *Proc. AIAA Guidance, Navigation and Control Conf.*, Toronto, Ontario, Aug. 2010, AIAA-2010-8344.

A Rest-to-Rest Reduced-Attitude Maneuver

We construct a rest-to-rest reduced-attitude maneuver that aligns the third principal axis of the body frame with the third axis of the inertial frame. This reduced-attitude maneuver transfers the initial reduced attitude $\Gamma_0 = R(0)^\top e_3 = (0.9097, 0.4097, 0.0670)$ to the terminal reduced attitude $\Gamma_f = (0, 0, 1)$ in a maneuver time of $T = 5$ s. The axis and angle variables are given as $a = (0.9118, -0.4107, 0)$ and $\alpha = 1.5038$ rad, respectively. Expressions for the reduced attitude, the angular velocity, and the control input that satisfy the specified boundary conditions are given by (15)–(17). In this instance, the rotation angle is $\theta(t) = (\alpha/2)(1 - \cos((\pi/T)t))$ rad.

The full-attitude maneuver studied above also satisfies the boundary conditions imposed for the reduced-attitude maneuver for the specified initial full rigid-body attitude. Since the reduced-attitude maneuver is less constrained than the full-attitude maneuver, it typically requires less control effort. For this rest-to-rest reduced-attitude maneuver, Figure 2 gives the (a) time responses of the principal angle, (b) norm of the angular velocity, and (c) norm of the control torque, all plotted versus normalized time. Figure 2(d) shows the reduced-attitude vector components versus normalized time for this maneuver. Figure 3 gives three snapshots of the reduced-attitude configuration, and the path traced out on the two-sphere at different instants in this maneuver, including the initial and final time instants. In Figure 3, the axes shown in the snapshots of the reduced-attitude maneuvers are the body axes.

Full-Attitude Stabilization

We construct a feedback controller that asymptotically aligns the three principal axes of the rigid body with the three inertial axes. Thus the desired attitude R_d is the identity matrix. The feedback controller is given by (22), where we select the vector $a = (1, 2, 3)$, and the nominal gains $K_p = \mathrm{diag}(1, 2, 3)$ and $K_v = \mathrm{diag}(5, 10, 15)$.

The closed-loop eigenvalues of the linearized closed-loop system at the equilibrium $(R_\mathrm{d}, 0)$ are given by $\{-14.3739, -9.1231, -3.618, -1.382, -0.8769, -0.6261\}$, thereby describing the local convergence rate near the desired equilibrium. The system has three additional equilibria corresponding to the attitudes $\{\mathrm{diag}(1, -1, -1), \mathrm{diag}(-1, -1, 1), \mathrm{diag}(-1, 1, -1)\}$ as described by (28)–(30) in Proposition 1.

We refer to the gains given above as defining a nominal controller. Two alternative sets of gains define a *stiff* controller and a *damped* controller. The stiff gains are obtained by increasing K_p and decreasing K_v by 25% each. In a similar manner, the damped gains are obtained by decreasing K_p and increasing K_v by 25% each. In each case, the desired full-attitude equilibrium $(R_\mathrm{d}, 0)$ is almost globally asymptotically stable on $\mathrm{SO}(3) \times \mathbb{R}^3$.

The three sets of gains yield nominal, stiff, and damped closed-loop responses locally near the desired equilibrium. These closed-loop responses are shown in Figure 4 for the initial conditions

$$\omega(0) = \begin{bmatrix} 0 \\ 0 \\ 0 \end{bmatrix}, \; R(0) = \begin{bmatrix} 0.2887 & 0.4082 & -0.8660 \\ -0.8165 & 0.5774 & 0 \\ 0.5000 & 0.7071 & 0.5000 \end{bmatrix}. \quad (51)$$

The error in the attitude is represented by the eigenangle

$$\Theta(t) = \cos^{-1}\frac{1}{2}(\mathrm{trace}(R(t)) - 1), \quad (52)$$

which is a scalar measure of the error between R and I. Thus, $\Theta(0) = 80°$. From Figure 4(a), we see that, compared to the nominal controller, the stiff controller acts

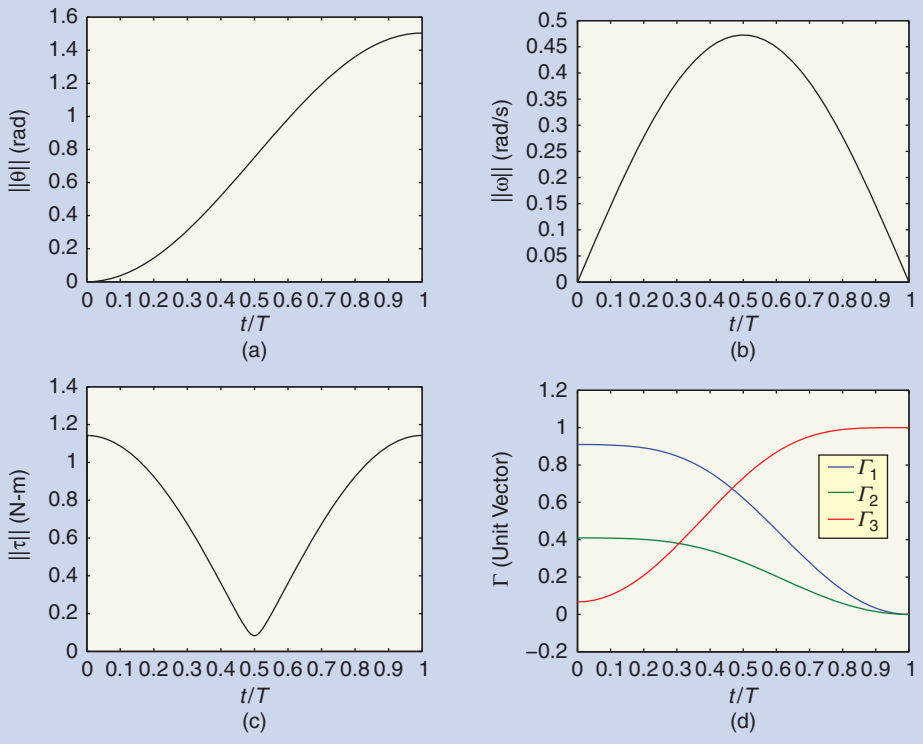

FIGURE 2 (a) Principal angle, (b) norm of angular velocity, (c) norm of the control torque, and (d) components of the reduced-attitude vector versus normalized time for the rest-to-rest reduced-attitude open-loop maneuver for a rigid body with inertia matrix $J = \text{diag}(3, 4, 5)$ kg-m^2, within the maneuver time $T = 5$ s. The reduced-attitude vector is the direction of the third principal axis of the rigid body, and the maneuver aligns the reduced-attitude vector with the third coordinate axis of the inertial coordinate frame. The principal axis of rotation is the cross product of the given initial reduced attitude $\Gamma(0)$ and the desired final reduced attitude $\Gamma(T)$, while the principal angle $\theta(t)$ is obtained by a sinusoidal interpolation between the boundary conditions. The angular-velocity and control-torque profiles are obtained from the principal angle and the resulting reduced-attitude profile. Although the norms of the angular-velocity and control-torque profiles look similar in shape to the corresponding profiles for the full-attitude maneuver, their values are considerably lower.

faster in reducing the error to zero, while the damped controller is slower in its response. However, as shown in Figure 4(b) and (c), the stiff controller requires a higher control torque and also leads to larger transient angular velocities compared to the nominal controller, while the damped controller requires less control torque and has lower transient angular velocities. The parameters a_1, a_2, and a_3 distribute the control effort among the three body axes, and these gains can be modified accordingly based on the moment of inertia and the desired response.

To illustrate the closed-loop performance limitations, we consider the linearization of the closed-loop system, as given in (44) for the nominal gains, at the unstable equilibrium corresponding to the attitude $R_\gamma = \text{diag}(-1, 1, -1)$. The local closed-loop dynamics near this unstable equilibrium are described by the positive eigenvalues $(0.1882, 0.6375)$, and negative eigenvalues $(-0.2324, -1.4343, -3.1882, -3.1375)$. These eigenvalues confirm that the equilibrium $(R_\gamma, 0)$ is unstable, and the stable manifold has dimension four, while the unstable manifold is two dimensional. The eigenspaces corresponding to the negative and positive eigenvalues are tangent to the stable and unstable manifolds at the equilibrium $(R_\gamma, 0)$.

To demonstrate performance limitations, we choose a family of initial conditions that lie close to the stable manifold of the unstable equilibrium $(R_\gamma, 0)$. We choose $v_a = [\Delta\Theta_a \;\; \Delta\omega_a]$ and $v_b = [\Delta\Theta_b \;\; \Delta\omega_b]$ as a linear combination of eigenvectors from the stable and unstable eigenspaces, respectively, of the equilibrium $(R_\gamma, 0)$, where

$$\Delta\Theta_a = \begin{bmatrix} 0.4021 \\ 0.3037 \\ 0.2993 \end{bmatrix}, \; \Delta\omega_a = \begin{bmatrix} 0.5939 \\ -0.9528 \\ -0.9542 \end{bmatrix},$$

$$\Delta\Theta_b = \begin{bmatrix} 0 \\ 0.8432 \\ 0.9827 \end{bmatrix}, \; \Delta\omega_b = \begin{bmatrix} 0 \\ 0.5375 \\ 0.1849 \end{bmatrix}.$$

Consider the initial conditions

$$R(0) = \text{diag}(-1, 1, -1)\exp(\delta\Delta\Theta_a^\times + \varepsilon\Delta\Theta_b^\times), \tag{53}$$

$$\omega(0) = \delta\Delta\omega_a + \varepsilon\Delta\omega_b, \tag{54}$$

which depends on the parameter ε. If we choose $0 < \delta \ll 1$, then, for $\varepsilon = 0$, Figure 5 shows that the initial conditions

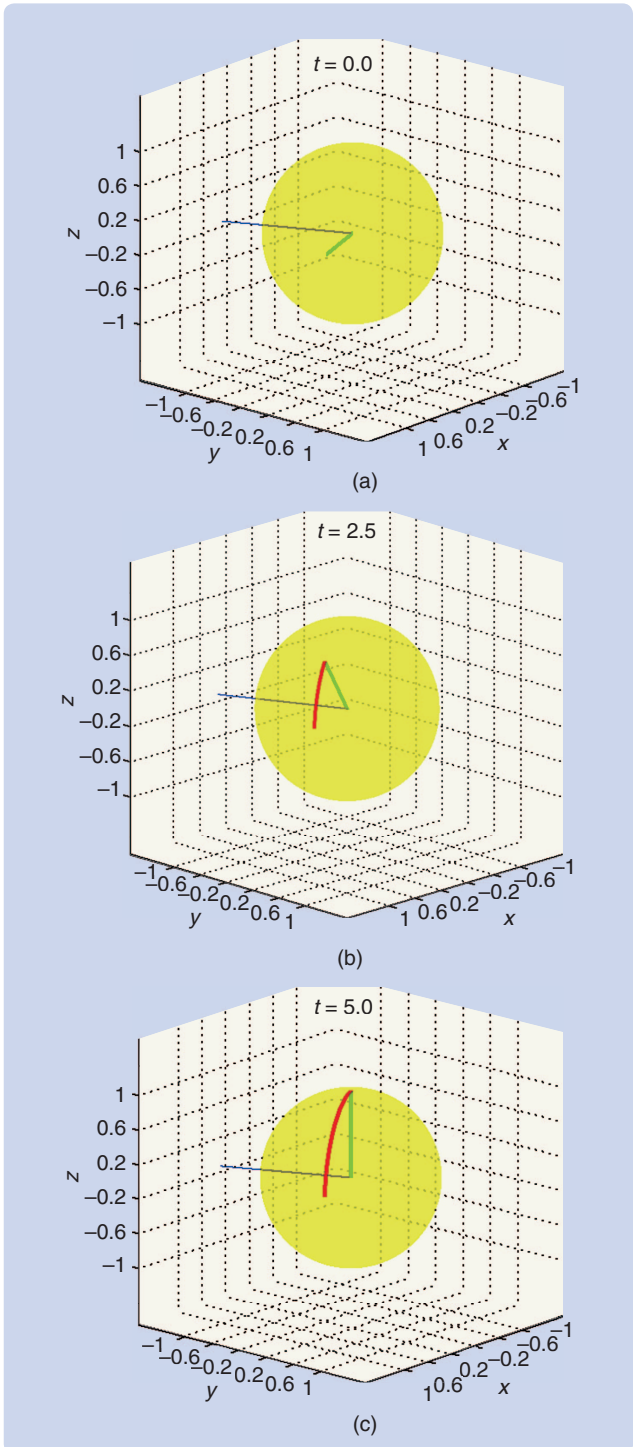

FIGURE 3 Snapshots of the rest-to-rest, open-loop, reduced-attitude maneuver for a rigid body with inertia matrix $J = \text{diag}(3, 4, 5)$ kg-m^2. The reduced-attitude vector is denoted by a bold green line from the origin to a point on the surface of the two-sphere. The path traced by the tip of the reduced-attitude vector on the two-sphere at several instants during the maneuver time $T = 5$ s is given by a bold red line. The principal axis of rotation, which is inertially fixed, is given by the blue line. The indicated axes are the body axes and not the inertial axes. (a) shows the initial reduced attitude, (b) is the reduced attitude at time $t = 2.5$ s, and (c) is the final reduced attitude at time $t = 5$ s.

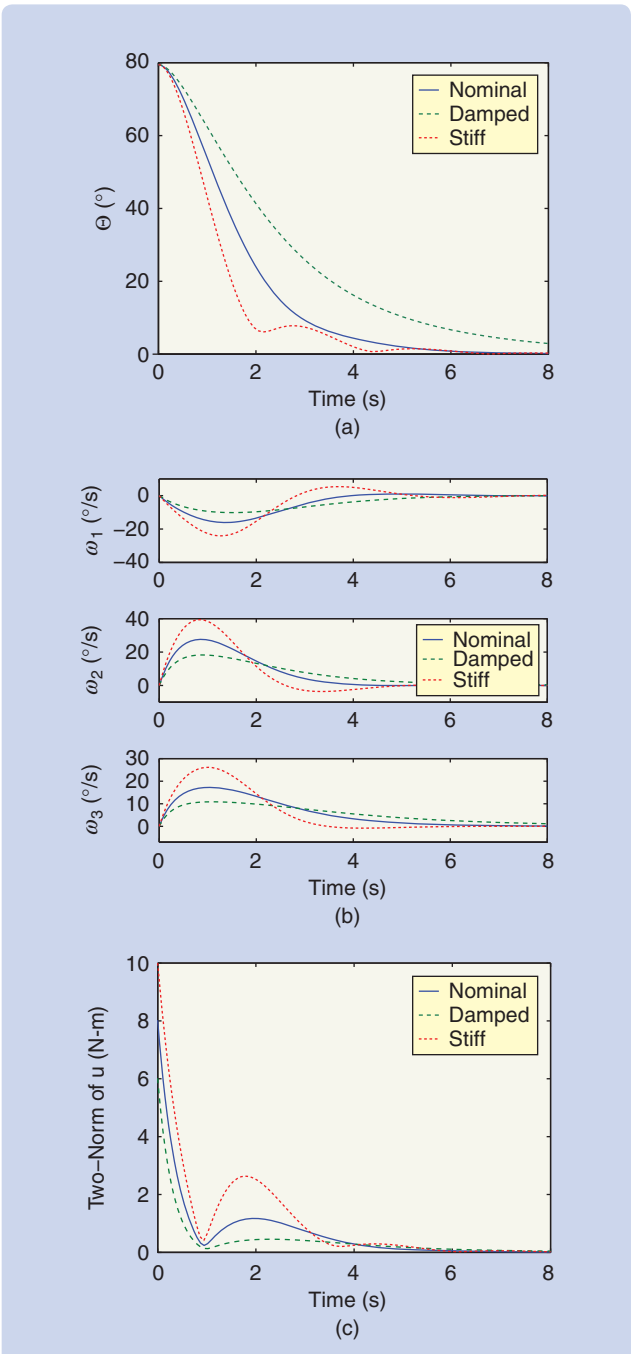

FIGURE 4 (a) Eigenangle, (b) angular velocity components along each body-fixed axis, and (c) the two-norm of the control torque are plotted for three controllers, namely, a nominal controller, a stiff controller, and a damped controller. As shown in (a), the error converges to zero faster in the case of the stiff controller since the gain K_p that acts on the error is 25% larger than the nominal controller. On the other hand, the error converges more slowly for the damped controller where the gain K_p is 25% lower than the nominal case. While the stiff controller yields faster convergence, the angular velocity as shown in (b) has larger transients in the case of the stiff controller compared to the nominal or damped controller. Furthermore, as shown in (c), the magnitude of the torque for the stiff controller is higher than the nominal controller, while the magnitude of the control torque is lower for the damped controller.

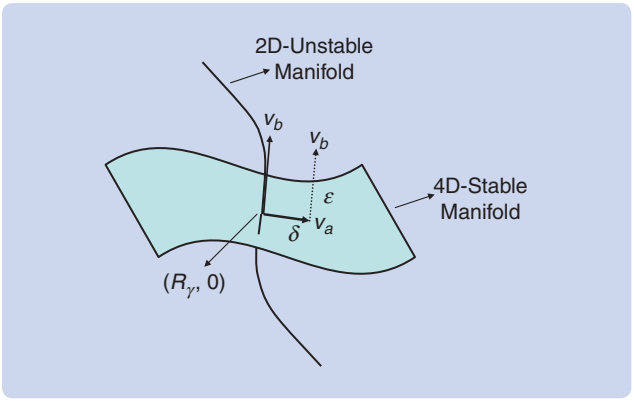

FIGURE 5 Initial conditions to illustrate closed-loop performance limitations. The unstable equilibrium $(R\gamma, 0)$ has a four-dimensional stable manifold and a two-dimensional unstable manifold. The vectors v_a and v_b are tangent to the stable and the unstable manifolds, respectively, at $(R_\gamma, 0)$. The initial conditions are perturbations from $(R_\gamma, 0)$ such that, for $\varepsilon = 0$, the initial condition lies close to the stable manifold, and, as ε increases, the initial condition lies farther away from the stable manifold. A fixed nonzero δ guarantees that the initial condition is near but not exactly at the equilibrium $(R_\gamma, 0)$ for every sufficiently small ε.

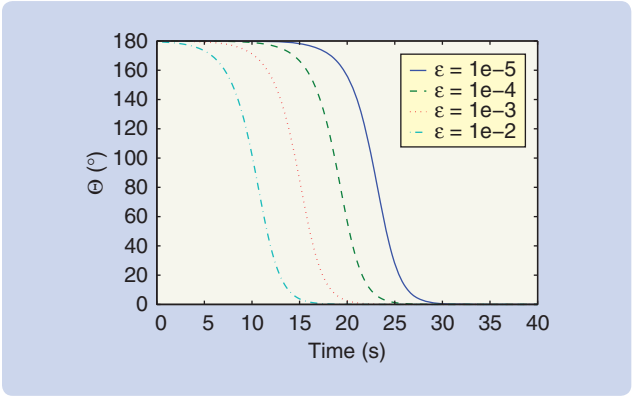

FIGURE 6 The error $\Theta(t)$ for the nominal controller for four initial conditions corresponding to four different values of ε in (53) and (54). The time for the error to converge to zero increases as ε is decreased. Most of the increase in the transient time occurs in the early part of the trajectory, where the scalar error is close to 180°. This behavior indicates that, as ε decreases, the trajectory dwells close to the unstable equilibrium $(R_\gamma, 0)$ and hence close to the error of 180°, since the solution starts closer to the four-dimensional stable manifold as illustrated in Figure 5. However, since the initial condition does not lie on the stable manifold, it soon diverges along the two-dimensional unstable manifold, finally converging to the desired equilibrium $(R_d, 0)$. The divergence along the unstable manifold results in a sharp drop in the attitude error to zero as shown above. The smaller the parameter ε, the longer the trajectories dwell close to the unstable equilibrium $(R_\gamma, 0)$.

(53), (54) lie close to the stable manifold of the unstable equilibrium. As ε increases, the distance to the stable manifold of the unstable equilibrium $(R_\gamma, 0)$ increases. Therefore, as ε decreases, we expect the time of convergence to the desired attitude $R_d = I$ to increase. Note that if v_a is not zero, then, whether or not $\varepsilon = 0$, the initial conditions (53), (54) lie close to the stable manifold but never exactly at the equilibrium $(R_\gamma, 0)$. In the simulations, we choose $\delta = 10^{-4}$.

In Figure 6, we plot the scalar attitude error given by the eigenangle (52) for four initial conditions corresponding to four different values of ε in (53) and (54) given by $\varepsilon \in \{10^{-5}, 10^{-4}, 10^{-3}, 10^{-2}\}$. As shown in Figure 6, the time of convergence increases with decreasing values of ε. Furthermore, the increase in the transient period occurs when the attitude error is near 180°, indicating that the solutions remain close to the unstable equilibrium $(R_\gamma, 0)$ for an extended period. This behavior demonstrates that the closer the solution starts to the complement of the domain of attraction of the desired equilibrium $(R_d, 0)$, the longer it takes for the solution to converge to $(R_d, 0)$.

Reduced-Attitude Stabilization

We construct a feedback controller that asymptotically aligns the third principal axis of the body frame with the third axis of the inertial frame. Thus, $b = (0, 0, 1)$, and the goal is to asymptotically stabilize $\Gamma_d = (0, 0, 1)$, that is, to asymptotically align $\Gamma = R^\top b$ with Γ_d. The feedback controller, given by (48), is chosen to have the gains $K_v = \mathrm{diag}(5, 10, 15)$ and $k_p = 4$.

The closed-loop eigenvalues of the linearized closed-loop system at $(\Gamma_d, 0)$ are given by $\{-0.8333 \pm 0.7993i, -0.5, -2, -3\}$, thereby describing the local convergence rate near the desired equilibrium. There also exists one additional equilibrium given by $(-\Gamma_d, 0)$ that is unstable.

We refer to the gains given above as defining a nominal controller. Two alternative sets of gains define a *stiff* controller and a *damped* controller. The stiff gains are obtained by increasing k_p and decreasing K_v by 25% each. In a similar manner, the damped gains are obtained by decreasing k_p and increasing K_v by 25% each. In each case, the desired reduced-attitude equilibrium $(\Gamma_d, 0)$ is almost globally asymptotically stable on $\mathbb{S}^2 \times \mathbb{R}^3$.

The three sets of gains yield nominal, stiff, and damped closed-loop responses locally near the desired equilibrium. Closed-loop responses are plotted in Figure 7 for the same initial conditions as above for the full-attitude case. Thus the initial condition for the reduced attitude is $\Gamma(0) = R(0)^\top e_3 = (0.5, 0.7071, 0.5)$. The error in the reduced attitude is

$$\Theta(t) = \cos^{-1}(\Gamma_d^\top \Gamma(t)), \tag{55}$$

which is a scalar measure of the error between Γ and Γ_d representing the angle between the two unit vectors. Thus, $\Theta(0) = 60°$. From Figure 7(a), we see that, compared to the nominal controller, the stiff controller is faster in reducing the error to zero, while the damped controller is slower in its response. However, as shown in Figure 7(b) and (c), the stiff

controller requires a higher control torque and also leads to larger transient angular velocities compared to the nominal controller, while the damped controller requires less control torque and has lower transient angular velocities.

To illustrate performance limitations in reduced-attitude feedback, we consider the linearization of the closed-loop system for the nominal controller about the unstable equilibrium $(-\Gamma_d, 0)$. It can be shown that the linearized closed-loop dynamics are described by the positive eigenvalues $(0.3508, 0.5907)$ and the negative eigenvalues $(-2.2573, -2.8508, -3)$. These eigenvalues indicate that the equilibrium at $(-\Gamma_d, 0)$ is unstable, and the stable manifold has dimension three, while the unstable manifold is two dimensional. The eigenspaces corresponding to the negative and positive eigenvalues are tangent to the stable and unstable manifolds at the equilibrium $(-\Gamma_d, 0)$.

To demonstrate performance limitations, we choose a family of initial conditions that lie close to the stable manifold of the unstable equilibrium $(-\Gamma_d, 0)$. We choose $v_a = [\Delta\Theta_a \;\; \Delta\omega_a]$ and $v_b = [\Delta\Theta_b \;\; \Delta\omega_b]$ as a linear combination of eigenvectors from the stable and unstable eigenspaces, respectively, of the equilibrium $(-\Gamma_d, 0)$, where

$$\Delta\Theta_a = \begin{bmatrix} 0 \\ 0 \\ -0.3162 \end{bmatrix}, \; \Delta\omega_a = \begin{bmatrix} 0 \\ 0 \\ 0.9487 \end{bmatrix},$$

$$\Delta\Theta_b = \begin{bmatrix} 0.8610 \\ 0 \\ 0 \end{bmatrix}, \; \Delta\omega_b = \begin{bmatrix} 0.5086 \\ 0 \\ 0 \end{bmatrix}.$$

Consider the family of initial conditions

$$\Gamma(0) = \exp(-\delta\Delta\Theta_a^{\times} - \varepsilon\Delta\Theta_b^{\times})(-\Gamma_d), \tag{56}$$

$$\omega(0) = \delta\Delta\omega_a + \varepsilon\Delta\omega_b, \tag{57}$$

which depend on the parameter ε.

If we choose $0 < \delta \ll 1$, then, for $\varepsilon = 0$, the initial conditions (56), (57) lie close to the stable manifold of the unstable equilibrium $(-\Gamma_d, 0)$. As ε increases, the distance to the stable manifold of the unstable equilibrium $(-\Gamma_d, 0)$ increases. Therefore, as ε decreases, we expect the time of convergence to the desired attitude Γ_d to increase. Note that, if v_a is not zero, then, whether or not $\varepsilon = 0$, the initial conditions (56), (57) lie close to the stable manifold but never exactly at the equilibrium $(-\Gamma_d, 0)$. In the simulations, we choose $\delta = 10^{-4}$.

In Figure 8, we plot the scalar reduced-attitude error defined in (55) for four initial conditions corresponding to values of ε in (56) and (57) given by $\varepsilon \in \{10^{-5}, 10^{-4}, 10^{-3}, 10^{-2}\}$. As shown in Figure 8, the time of convergence increases as ε decreases. Furthermore, the increase in the transient period occurs when the reduced-attitude error is near 180°, indicating that the solutions remain close to the unstable equilibrium $(-\Gamma_d, 0)$ for an extended period. This

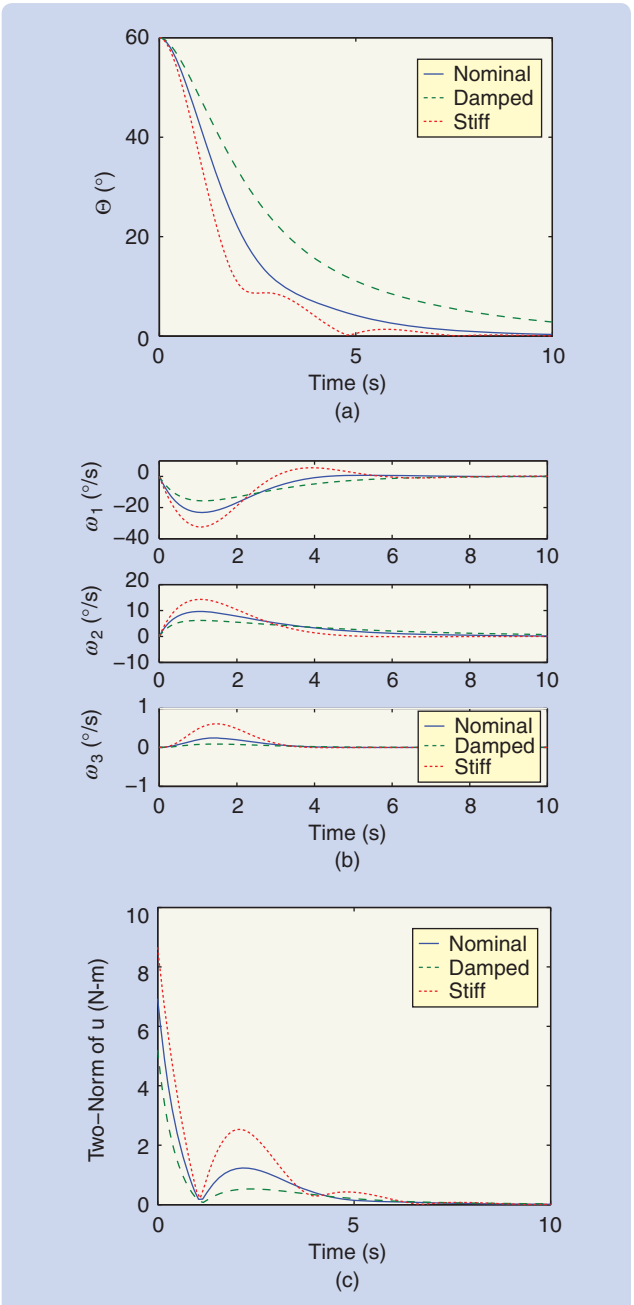

FIGURE 7 (a) The angle between the desired and actual reduced-attitude vectors, (b) angular velocity components along each body-fixed axis, and (c) the two-norm of the control torque plotted for three controllers, namely, a nominal controller, a stiff controller, and a damped controller. As shown in (a), the error converges to zero faster in the case of a stiff controller since the gain k_p that acts on the error is 25% larger than the nominal controller. On the other hand, the error converges more slowly for the damped controller, where the gain k_p is 25% lower than the nominal case. While the stiff controller yields faster convergence, the angular velocity as shown in (b) has larger transients in the case of the stiff controller compared to the nominal and damped controllers and hence can excite unmodeled dynamics. Furthermore, as shown in (c), the magnitude of the torque for the stiff controller is higher than the nominal controller, while the magnitude of the control torque is lower for the damped controller.

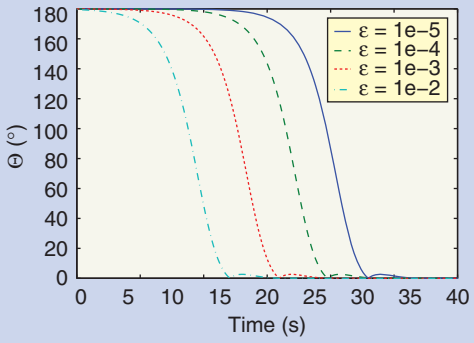

FIGURE 8 The error $\Theta(t)$ for the nominal controller for four initial conditions corresponding to four different values of ε in (56) and (57). The time for the error to converge to zero increases as ε is decreased. Most of this increase in the transient time occurs in the early part of the trajectory, where the scalar error is close to 180°. This behavior indicates that, as ε decreases, the trajectory dwells close to the unstable equilibrium $(-\Gamma_d, 0)$, and hence close to the error of 180°, since the solution starts closer to the three-dimensional stable manifold. However, since the initial condition does not lie on the stable manifold, it soon diverges along the two-dimensional unstable manifold, finally converging to the desired reduced-attitude equilibrium $(\Gamma_d, 0)$. The divergence along the unstable manifold results in a sharp drop in the attitude error to zero as shown above. The smaller the parameter ε, the longer the trajectories dwell close to the unstable equilibrium manifold.

example illustrates that the closer the solution starts to the complement of the domain of attraction, the longer it takes to converge to $(\Gamma_d, 0)$.

CONCLUSIONS

This article summarizes global results on attitude control and stabilization for a rigid body using continuous time-invariant feedback. The analysis uses methods of geometric mechanics based on the geometry of the special orthogonal group $\mathrm{SO}(3)$ and the two-sphere $\mathbb{S}^2$.

We construct control laws for full- and reduced-attitude maneuvers for arbitrary given boundary conditions and an arbitrary maneuver time. These results demonstrate controllability properties for both the full- and for reduced-attitude models, assuming full actuation. The open-loop controllers have a discontinuous dependence on the boundary conditions, thus suggesting the impossibility of global stabilization using continuous feedback.

Both full- and reduced-attitude feedback stabilization results are provided, assuming full actuation. Since no continuous time-invariant feedback controller can achieve global asymptotic stabilization of an equilibrium, global properties of the closed-loop attitude dynamics using the continuous feedback controllers (22) and (48) are characterized. The particular feedback controllers given here are globally defined and continuous, and they achieve almost-global full-attitude stabilization or almost-global reduced-attitude stabilization in the sense that the complement of the domain of attraction lies in a lower dimensional set of the state space that is nowhere dense. Some features of the geometry of the complement of the domain of attraction of the desired equilibrium are described, identifying it as the union of the undesired closed-loop equilibria and their associated stable manifolds. A key aspect of the analysis given in this article is that we perform both local and global analysis of the feedback controllers without resorting to coordinates for $\mathrm{SO}(3)$ or $\mathbb{S}^2$.

ACKNOWLEDGMENTS

We appreciate the many conversations and suggestions made by Taeyoung Lee and Melvin Leok, who helped to clarify some of the attitude control issues addressed in this article. We also thank the reviewers for suggestions that helped to improve the presentation of this article.

AUTHOR INFORMATION

Nalin A. Chaturvedi (nalin.chaturvedi@us.bosch.com) is a senior research engineer at the Research and Technology Center of the Robert Bosch LLC, Palo Alto, California. He received the B.Tech. and the M.Tech. in aerospace engineering from the Indian Institute of Technology, Bombay, in 2003, receiving the Institute Silver Medal. He received the M.S. in mathematics and the Ph.D. in aerospace engineering from the University of Michigan, Ann Arbor, in 2007. He was awarded the Ivor K. McIvor Award in recognition of his research in applied mechanics. His current interests include the development of model-based control for complex physical systems involving thermal-chemical-fluid interactions, nonlinear dynamical systems, state and parameter estimation, and adaptive control with applications to systems governed by PDE, nonlinear stability theory, geometric mechanics, and nonlinear control. He is a member of the Energy Systems subcommittee within the Mechatronics technical committee of the ASME Dynamic Systems and Controls Division and an associate editor on the IEEE Control Systems Society Editorial Board. He is a visiting scientist at the University of California, San Diego. He can be contacted at Robert Bosch LLC, Research and Technology Center, 4005 Miranda Avenue, Suite 200, Palo Alto, CA 94304 USA.

Amit K. Sanyal received the B.Tech. in aerospace engineering from the Indian Institute of Technology, Kanpur, in 1999. He received the M.S. in aerospace engineering from Texas A&M University in 2001, where he obtained the Distinguished Student Masters Research Award. He received the M.S. in mathematics and Ph.D. in aerospace engineering from the University of Michigan in 2004. From 2004 to 2006, he was a postdoctoral research associate in the Mechanical and Aerospace Engineering Department at Arizona State University. From 2007 to 2010, he was an assistant professor in mechanical engineering at the University of Hawaii and is currently an assistant professor in mechanical and aerospace engineering at

New Mexico State University. His research interests are in geometric mechanics, geometric control, discrete variational mechanics for numerical integration of mechanical systems, optimal control and estimation, geometric/algebraic methods applied to nonlinear systems, spacecraft guidance and control, and control of unmanned vehicles. He is a member of the IEEE Control Systems Society Technical Committee on Aerospace Control and the AIAA Guidance, Navigation, and Control Technical Committee.

N. Harris McClamroch received the Ph.D. in engineering mechanics from the University of Texas at Austin. Since 1967 he has been with the University of Michigan, Ann Arbor, Michigan, where he is a professor emeritus in the Department of Aerospace Engineering. During the past 25 years, his primary research interest has been in nonlinear control. He has worked on control engineering problems arising in robotics, automated systems, and aerospace flight systems. He is a Fellow of the IEEE, received the IEEE Control Systems Society Distinguished Member Award, and is a recipient of the IEEE Third Millennium Medal. He has served as an associate editor and editor of *IEEE Transactions on Automatic Control*, and he has held numerous positions in the IEEE Control Systems Society, including president.

REFERENCES

[1] M. D. Shuster, "A survey of attitude representations," *J. Astronaut. Sci.*, vol. 41, no. 4, pp. 439–517, 1993.

[2] J. Stuelpnagel, "On the parameterization of the three-dimensional rotation group," *SIAM Rev.*, vol. 6, no. 4, pp. 422–430, 1964.

[3] R. E. Mortensen, "A globally stable linear attitude regulator," *Int. J. Control*, vol. 8, no. 3, pp. 297–302, 1968.

[4] B. Wie and P. M. Barba, "Quaternion feedback for spacecraft large angle maneuvers," *AIAA J. Guid. Control Dyn.*, vol. 8, no. 3, pp. 360–365, 1985.

[5] B. Wie, H. Weiss, and A. Arapostathis, "Quaternion feedback regulator for spacecraft eigenaxis rotation," *J. Guid. Control Dyn.*, vol. 12, pp. 375–380, 1989.

[6] J. T. Wen and K. K. Delgado, "The attitude control problem," *IEEE Trans. Automat. Cont.*, vol. 36, no. 10, pp. 1148–1162, 1991.

[7] R. Bach and R. Paielli, "Linearization of attitude-control error dynamics," *IEEE Trans. Automat. Cont.*, vol. 38, no. 10, pp. 1521–1525, 1993.

[8] S. M. Joshi, A. G. Kelkar, and J. T.-Y. Wen, "Robust attitude stabilization of spacecraft using nonlinear quaternion feedback," *IEEE Trans. Automat. Cont.*, vol. 40, no. 10, pp. 1800–1803, 1995.

[9] S. P. Bhat and D. S. Bernstein, "A topological obstruction to continuous global stabilization of rotational motion and the unwinding phenomenon," *Syst. Control Lett.*, vol. 39, no. 1, pp. 63–70, 2000.

[10] P. C. Hughes, *Spacecraft Attitude Dynamics*. New York: Wiley, 1986.

[11] B. Wie, *Spacecraft Vehicle Dynamics and Control*. Reston, VA: AIAA, 1998.

[12] G. Meyer, "Design and global analysis of spacecraft attitude control systems," NASA Tech. Rep. R-361, Mar. 1971.

[13] P. E. Crouch, "Spacecraft attitude control and stabilization: Applications of geometric control theory to rigid body models," *IEEE Trans. Automat. Contr.*, vol. 29, no. 4, pp. 321–331, 1984.

[14] F. Bullo, R. M. Murray, and A. Sarti, "Control on the sphere and reduced attitude stabilization," in *Proc. IFAC Symp. Nonlinear Control Systems*, Tahoe City, CA, 1995, vol. 2, pp. 495–501.

[15] P. Tsiotras and J. M. Longuski, "Spin-axis stabilization of symmetrical spacecraft with two control torques," *Syst. Control Lett.*, vol. 23, no. 6, pp. 395–402, 1994.

[16] D. E. Koditschek, "The application of total energy as a Lyapunov function for mechanical control systems," in *Proc. AMS-IMS-SIAM Joint Summer Research Conf.*, Bowdin College, Maine, 1988, vol. 97, pp. 131–157. *Dynamics and Control of Multibody Systems*, J. E. Marsden, P. S. Krishnaprasad, and J. C. Simo, Eds. Providence, RI: American Mathematical Society.

[17] S. Bharadwaj, M. Osipchuk, K. D. Mease, and F. Park, "A geometric approach to global attitude stabilization," in *Proc. AIAA/AAS Astrodynamics Specialist Conf.*, San Diego, 1996, pp. 806–816.

[18] S. Bharadwaj, M. Osipchuk, K. D. Mease, and F. C. Park, "Geometry and inverse optimality of global attitude stabilization," *J. Guid. Control Dyn.*, vol. 21, no. 6, pp. 930–939, 1998.

[19] N. A. Chaturvedi, F. Bacconi, A. K. Sanyal, D. S. Bernstein, and N. H. McClamroch, "Stabilization of a 3D rigid pendulum," in *Proc. American Control Conf.*, Portland, OR, 2005, pp. 3030–3035.

[20] N. A. Chaturvedi and N. H. McClamroch, "Global stabilization of an inverted 3D pendulum including control saturation effects," in *Proc. 45th IEEE Conf. Decision and Control*, San Diego, CA, Dec. 2006, pp. 6488–6493.

[21] N. A. Chaturvedi, N. H. McClamroch, and D. S. Bernstein, "Stabilization of a specified equilibrium in the inverted equilibrium manifold of the 3D pendulum," in *Proc. American Control Conf.*, 2007, pp. 2485–2490.

[22] N. A. Chaturvedi and N. H. McClamroch, "Asymptotic stabilization of the hanging equilibrium manifold of the 3D pendulum," *Int. J. Robust Nonlinear Control*, vol. 17, no. 16, pp. 1435–1454, 2007.

[23] N. A. Chaturvedi, N. H. McClamroch, and D. S. Bernstein, "Asymptotic smooth stabilization of the inverted 3D pendulum," *IEEE Trans. Automat. Contr.*, vol. 54, no. 6, pp. 1204–1215, 2009.

[24] W. Kang, "Nonlinear H-infinity control and its application to rigid spacecraft," *IEEE Trans. Automat. Contr.*, vol. 40, no. 7, pp. 1281–1285, 1995.

[25] A. K. Sanyal and N. A. Chaturvedi, "Almost global robust attitude tracking control of spacecraft in gravity," in *Proc. AIAA Conf. Guidance, Navigation, and Control*, Honolulu, HI, Aug. 2008, AIAA-2008-6979.

[26] A. K. Sanyal, A. Fosbury, N. A. Chaturvedi, and D. S. Bernstein, "Inertia-free spacecraft attitude trajectory tracking with disturbance rejection and almost global stabilization," *AIAA J. Guid. Control Dyn.*, vol. 32, pp. 1167–1178, 2009.

[27] N. A. Chaturvedi and N. H. McClamroch, "Asymptotic stabilization of the inverted equilibrium manifold of the 3D pendulum using non-smooth feedback," *IEEE Trans. Automat. Contr.*, vol. 54, no. 11, pp. 2658–2662, 2009.

[28] J. L. Junkins and J. D. Turner, *Optimal Spacecraft Rotational Maneuvers*. New York: Elsevier, 1986.

[29] M. J. Sidi, *Spacecraft Dynamics and Control—A Practical Engineering Approach*. Cambridge, U.K.: Cambridge Univ. Press, 2000.

[30] J. Shen, A. K. Sanyal, N. A. Chaturvedi, D. S. Bernstein, and N. H. McClamroch, "Dynamics and control of a 3D pendulum," in *Proc. IEEE Conf. Decision and Control*, Bahamas, 2004, pp. 323–328.

[31] N. A. Chaturvedi, T. Y. Lee, M. Leok, and N. H. McClamroch, "Nonlinear dynamics of the 3D pendulum," *J. Nonlinear Sci.*, vol. 21, no. 1, pp. 3–32, 2011.

[32] N. A. Chaturvedi, N. H. McClamroch, and D. S. Bernstein, "Stabilization of a 3D axially symmetric pendulum," *Automatica*, vol. 44, no. 9, pp. 2258–2265, 2008.

[33] P. Tsiotras, M. Corless, and J. Longuski, "A novel approach for the attitude control of an axisymmetric spacecraft subject to two control torques," *Automatica*, vol. 31, no. 8, pp. 1099–1112, 1995.

[34] A. M. Bloch, *Nonholonomic Mechanics and Control*. New York: Springer-Verlag, 2003.

[35] V. S. Varadarajan, *Lie Groups, Lie Algebras, and Their Representations*. New York: Springer-Verlag, 1984.

[36] R. M. Murray, Z. Li, and S. S. Sastry, *A Mathematical Introduction to Robotic Manipulation*. Boca Raton, FL: CRC Press, 1994.

[37] F. Bullo and A. D. Lewis, *Geometric Control of Mechanical Systems*. New York: Springer-Verlag, 2005.

[38] J. Guckenheimer and P. Holmes, *Nonlinear Oscillations, Dynamical Systems, and Bifurcations of Vector Fields*. New York: Springer-Verlag, 1983.

[39] C. G. Mayhew, R. G. Sanfelice, and A. R. Teel, "Robust global asymptotic attitude stabilization of a rigid body by quaternion-based hybrid feedback," in *Proc. 48th IEEE Conf. Decision and Control*, Shanghai, Dec. 2009, pp. 2522–2527.

[40] H. K. Khalil, *Nonlinear Systems*. Englewood Cliffs, NJ: Prentice-Hall, 2002.

[41] J. Cortés, "Discontinuous dynamical systems: A tutorial on solutions, nonsmooth analysis, and stability," *IEEE Control Syst. Mag.*, vol. 28, no. 3, pp. 36–73, 2008.